IOWA STATE UNIVERSITY
Digital Repository

Retrospective Theses and Dissertations

Iowa State University Capstones, Theses and Dissertations

2007

# Solar heating of a residential building in Kazakhstan

Ernar Aidargazaevich Makishev
*Iowa State University*

Follow this and additional works at: https://lib.dr.iastate.edu/rtd

 Part of the Civil Engineering Commons, Energy Systems Commons, Oil, Gas, and Energy Commons, and the Power and Energy Commons

Recommended Citation
Makishev, Ernar Aidargazaevich, "Solar heating of a residential building in Kazakhstan" (2007). *Retrospective Theses and Dissertations*. 15082.
https://lib.dr.iastate.edu/rtd/15082

This Thesis is brought to you for free and open access by the Iowa State University Capstones, Theses and Dissertations at Iowa State University Digital Repository. It has been accepted for inclusion in Retrospective Theses and Dissertations by an authorized administrator of Iowa State University Digital Repository. For more information, please contact digirep@iastate.edu.

www.manaraa.com

# Solar heating of a residential building in Kazakhstan

by

**Ernar Aidargazaevich Makishev**

A thesis submitted to the graduate faculty

in partial fulfillment of the requirements for the degree of

MASTER OF SCIENCE

Major: Mechanical Engineering

Program of Study Committee:
Michael B. Pate, Major Professor
Ron Nelson
Partha Sarkar

Iowa State University

Ames, Iowa

2007

www.manaraa.com

UMI Number: 1446118

UMI

UMI Microform 1446118

Copyright 2007 by ProQuest Information and Learning Company.
All rights reserved. This microform edition is protected against unauthorized copying under Title 17, United States Code.

ProQuest Information and Learning Company
300 North Zeeb Road
P.O. Box 1346
Ann Arbor, MI 48106-1346

www.manaraa.com

# TABLE OF CONTENTS



www.manaraa.com

www.manaraa.com

## LIST OF FIGURES



www.manaraa.com

www.manaraa.com

## LIST OF TABLES



www.manaraa.com

# 1. INTRODUCTION

The goal of this Master's thesis is to design a residential house in Astana, Kazakhstan, that does not consume energy for space heating from conventional power plants or autonomous power generators. Space heating is the largest part of energy consumption in cold climates. The primary source of energy chosen for this study is solar energy. A solar energy building is a subclass of the more general term "zero energy building."

The term "zero energy building" was coined by the Department of Energy of the United States as part of its program to design more efficient buildings. There are various names used across the literature pertaining to the same definition, including ‘green buildings’ and ‘passive housing.’

Usually when we hear the term "zero energy building," we may immediately visualize buildings equipped with alternative energy-harnessing devices. However, this term represents an even bigger area of alternative energy technology. Human waste utilization, for example, is in part zero energy technology.

Zero energy buildings must comply with stringent, specific criteria, such as:

- Exploiting alternative energy technology to supply energy needs;
- Reducing heat loss due to conduction through exterior materials;
- Diminishing water consumption and waste through more rational water use;
- Decreasing the amount of pollution produced by power plants for the heating and cooling of residential houses.

www.manaraa.com

In addition, there are many other criteria that are related to the environmental aspects of a building that are outside the scope of this thesis.

There is no part of the world that is not touched by rising energy costs. Even though Kazakhstan has tremendous amounts of energy available to it, the exportation of these sources is more profitable than fulfilling domestic market needs. Hence, the prices charged by energy carriers are increasing. Eventually, these prices will reach the point where alternative energy technologies, and solar energy technology in particular, will be affordable for the middle class. The potential of solar energy use is not limited to space heating. Solar cooling, water distillation, electric power generation, and many other fields ensure a promising future for solar energy.

Solar energy is an attractive area of alternative energy technologies research, not only because of its availability as an energy source and because of the high prices charged by conventional energy carriers, but also due to the fact that most other alternative energy technologies use energy sources that would not exist without solar energy (i.e., wind as the result of the asymmetrical heating of the atmosphere or biomass as the result of photosynthesis).

## 1.1. General Information

Kazakhstan, once a part of the USSR, is situated in the middle of Asia. According to the recent July 2006 census, the population is 15,233,244 people [1]. Astana (formerly Celinograd) was designated the capital of Kazakhstan in 1997. The following are the geographical coordinates of Astana: 51.18° N 71.45° E. Its elevation is

www.manaraa.com

at 1148 feet or /350m, which is relatively average. Ames, Iowa, for example, is 1158 ft / 353 m above the mean sea level.

There are 3 coal power plants in Astana [2]. Each one produces 110 Mw of electricity and provides residential space heating. The main type of heating is central heating with hot water from power plants being delivered to the buildings. The population of the city is 600,000 people, growing at a rate of 0.352 % (2007 est.) [2]. As a consequence of this, an energy shortage is expected in the future.

### 1.2. Climate

According to the Köppen Climate Classification System, the best description of Astana's type of climate is B s k, where B stands for arid climate, s stands for steppe and k stands for cold arid climate [3]. Even though January has the lowest average minimum temperature, Table 1 shows that February is the coldest month. From the engineering point of view these conditions complicate the implementation of solar technologies since the solar position in winter is low and the climate is harsh.

*Table 1: Design temperatures and wind speed for Astana, Kazakhstan [4].*

| Data | Value | f,% |
|---|---|---|
| Coldest month/Design temperature | 2/ -21.5 °C | |
| Wind speed, mph<br>k/h | 28.8<br>12.9 | 1 |
| Hottest month/Design temperature | 7/28.1 °C | |

Note: f is the annual cumulative frequency of occurrence.

www.manaraa.com

This climotological definition is geographically similar to most other interior locations of large land masses as Kazakhstan is situated in the middle of Eurasia and does not have marine access (except for the Caspian Sea, which does not flow directly into any international waters).

As we can see from Tables E.2 and E.3, the cooling load in the summer is not a significant part of the annual energy consumption; therefore, cooling loads are assumed to be negligible during the summer period.

### 1.3. Why there is a need for solar heating in a residential building

Kazakhstan has experienced a relatively high demographic increase since the fall of the Soviet Union. Economic improvement and a relatively stable political situation have encouraged people to obtain mortgages for new apartments. Therefore, there is a need for affordable housing for the growing population. Currently, most of the urban population lives in condominiums within the city limits.

Astana itself is a rapidly growing city (with an increase in population from 1997 to 2007 of 500 % [2]), and suburbs are only just starting to be developed. Future shortages in energy supplies and the above-mentioned boom in suburban development indicate a large potential market for alternative energy technologies such as solar space heating.

### 1.4. Model description used in this study

The model building is a typical American-style three-bedroom residential house [5]. The reason for choosing an American-style building is the efficiency of its

www.manaraa.com

construction. Most residential houses in Kazakhstan are built in the same way as they were 70 years ago: brick enveloped with poor inner insulation and low quality windows. They do not have ventilation or cooling systems. Uncontrolled infiltration and poor insulation design lead to uncomfortable conditions inside of these buildings. Conversely, American-style buildings (2x6 frames) show good results in reducing heating and cooling loads and providing comfortable conditions for their inhabitants. In addition, the absence of ventilation in Kazakhstan buildings increases the risk of radon contamination within the building [6]. A full description of the building is in Appendix D. Figures 1 to 4 show exterior of the building that is used in the simulation of solar space heating.

The heating area is:

1st = floor1534 $ft^2$

Unheated area (garage) = 791 $ft^2$

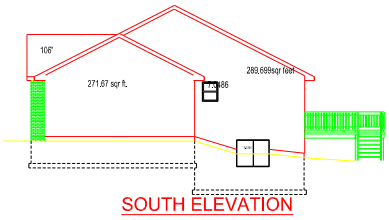


*Figure 1: South elevation*

www.manaraa.com

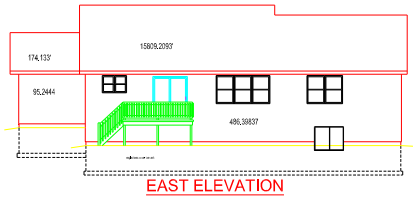


*Figure 2: East elevation*

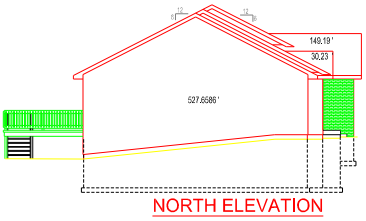


*Figure 3: North elevation*

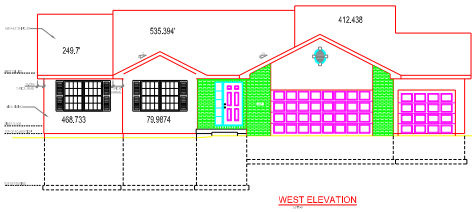


*Figure 4: West elevation*

www.manaraa.com

### 1.4.1. Heating loads

Heating loads are calculated using standard ASHRAE methods [6] for the calculation of heating loads for residential houses. The total exposed area of the house is listed in Appendix D.

ASHRAE methods use the following approximations [6]:

- The average wind speed is 15 mph;
- The temperature in uninsulated area is at the outdoor temperature;
- Disregard of the effects of rooms on heating load calculations;
- The unit leakage area (average construction type) [6];

$$A_{ul} = 0.04\left[\frac{in^2}{ft^2}\right] \quad (1.2)$$

The exposed surface area (gross wall area);

$$A_{es} = 2905\left[ft^2\right] \quad (1.2)$$

The average unit leakage area:

$$A_L = A_{es} \cdot A_{ul} \quad (1.3)$$

Where:

- $A_{es}$ is the building's exposed surface area, $ft^2$;
- $A_{ul}$ is the unit leakage area, $in^2 / ft^2$ .

Infiltration driving force can be calculated using following formula:

$$IDF = \frac{I_o + H \times \left|\Delta T\right| \times (I_1 + I_2 \times (\frac{A_{L,flue}}{A_L}))}{1000} \quad (1.4)$$

Where:

www.manaraa.com

- H is the building's average stack height, ft;
- $I_o, I_1, I_2$ are coefficients;
- $|\Delta T|$ is the difference between inside and outside air, K;
- $A_{L,flue}$ is the flue effective leakage area, ft;
- $A_L$ , is the average unit leakage area, ft.

*Table 2: Material characteristics [5]*

| Envelope | Insulation type |
|---|---|
| Basement walls | 2" rigid R10 Dow insulation on exterior; |
| 2x6 walls | R19 batts; |
| Attic | R46 blown fiberglass; |
| Windows | Low-e windows 'Pella'; |

Note: Window and door properties are specified on a floor plan.

Infiltration rate can be calculated by:

$$\text{ACH}=\frac{60\times(\text{A}_\text{L}\times IDF)}{V} \quad (1.5)$$

Where:

- ACH is air change per hour;
- V is the building volume, $ft^3$
- $A_L$ is the average unit leakage area, ft;

www.manaraa.com

- Infiltration driving force.

Required ventilation flow rate can be found as:

$$Q_v = 0.01 \times A_{cf} + 7.5 \times (N_{br} + 1) \quad (1.6)$$

Where:

- $A_{cf}$ is the building conditioned floor area, $ft^2$;
- $N_{br}$ is the number of bedrooms.

Heat losses through the building envelope are calculated by:

$$Q = U \cdot A \cdot \Delta T \quad (1.7)$$

Where:

- U is material conductivity, $\frac{BTU}{h \cdot ft^2 \cdot F}$;
- A is gross area, $m^2$;
- $\Delta T$ is the temperature difference between inside and outside air, F.

### 1.4.2 Radiation influence

The sun adds great amounts of energy to the heating loads; however, considering the severe climate conditions, this amount of energy can be disregarded to add reliability to the system.

### 1.5.3. Programming

A computer program that calculates heating loads has been developed to work with the main program of solar heating system simulation. This computer program is a

www.manaraa.com

'black-box' type of program. The only input parameter is the number of a month. The output is the heating load in BTU/h. A full listing of the program is a part of the main program in Appendix A. Heating loads are calculated for the heating season, which starts in October and ends in March. Since we do not have reliable daily temperature data, average temperatures have been used in the simulation.

www.manaraa.com

## 2. RADIATION DETERMINATION

In order to use solar energy, an estimation of the amount of solar energy that is incident on a particular location is essential. Solar energy that is incident on the Earth depends on several factors, such as solar trajectory, the change of seasons, atmospheric characteristics, and so on.

Solar trajectory has been studied since ancient times and precise methods have been developed to measure it. On the other hand, the atmospheric influence on solar radiation had not been researched until meteorology was established as a science in the nineteenth century.

The atmosphere acts as a protective shield against solar radiation. There are two major obstacles that determine the amount of energy that passes through the atmosphere: a) scattering and b) absorption. Scattering mostly occurs due to the interaction of radiation with air, water, and dust particles. The major effect of scattering is the result of the size of these particles. Increasing levels of air pollution limit solar energy incidence on the earth's surface.

The absorption of solar energy mostly occurs due to the absorption of radiation by the ozone layer. However, many other atmospheric components absorb solar energy as well. These components target certain wavelengths of solar radiation. While ozone tends to absorb ultraviolet radiation (wavelengths shorter than 0.29 $\mu m$ ), carbon dioxide and water vapor absorb infrared radiation.

www.manaraa.com

## 2.1. Actual data

The radiation data for Kazakhstan is obtained from the World Radiation Data Centre, which is maintained by the Russian Federal Service for Hydrometeorology and Environmental Monitoring.

The radiation measuring station closest to Astana is located in Semipalatinsk, which was the nuclear weapons testing area for the former USSR, located 500 km from the city. The coordinates of this station are at 50.21° N and 80.15° E while the elevation is 206 meters above sea level. The accessible data for this particular location are as follows:

- Global radiation, from 1964 to 1992;
- Diffuse radiation, from 1990-1993;
- The number of hours of sunshine, from 1962 to 1992;
- The net total radiation, from 1964 to 1992.

Global radiation is the total radiation (beam and diffuse) on a horizontal surface. Obviously, diffuse radiation is a part of global radiation; however, there is no information on the ground reflectivity of the measurement area, which influences diffuse radiation and other parameters of measurements. Figure 5 compares the mean monthly sums of global and diffuse radiation on a horizontal surface.

Net total radiation is the difference between global radiation on a horizontal surface and the amount of radiation emitted by the earth at this point. Net total radiation is measured by placing two pyranometers, one facing the earth and one facing the sky, in order to record the differences. This data is designated as meteorological study and is useless for radiation estimation in terms of solar energy usage.

www.manaraa.com

The number of hours of sunshine was measured by placing special paper next to a lens that burns into the paper, making a trace line of sunshine with respect to time.

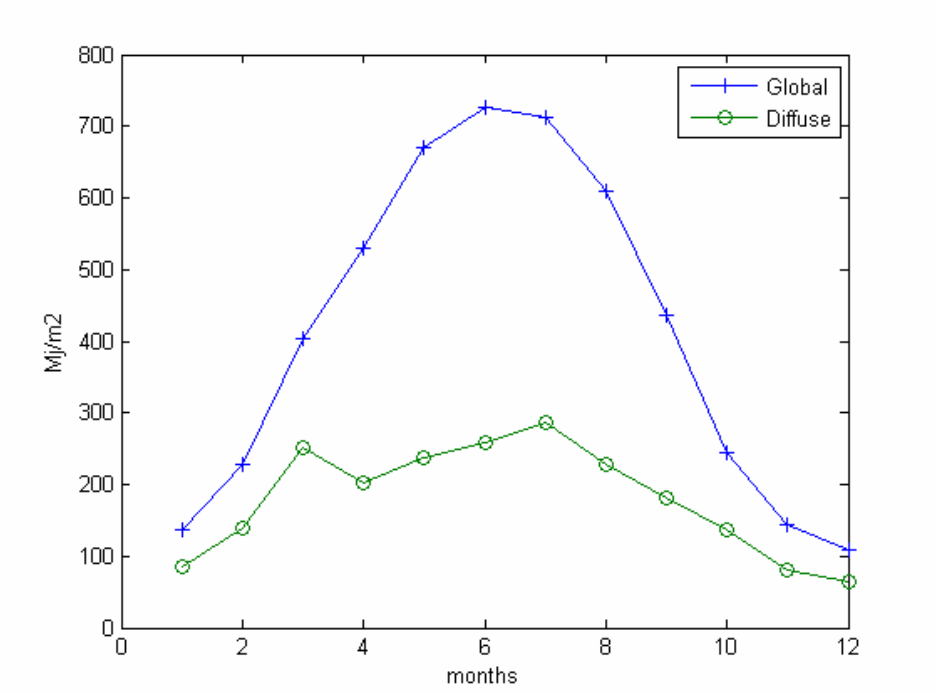


*Figure 5: Mean monthly sums of global and diffuse radiation on a horizontal surface (Data for diffuse radiation covers 2 years from 1990 to 1992, for global radiation covers 28 years from 1964 to 1992)*

An example of a data file is listed in Appendix B. The data is provided in the form of a text file with columns of numbers. The specification for the file explains particular numbers by their position in the line. There are several different specifications for different types of data. The first column of data file contains the type of data form, the location code, the date, and the radiation code. The radiation code is specified by the method by which radiation data were measured. The following columns depend on the data form and can be filled, for example, with the daily means of global radiation incidence on a horizontal surface in MJ/m2.

www.manaraa.com

The first challenge was collecting the data and studying the specification in order to decipher the data. The data is kept on perfo-cards, which can be understood by consideration of the format of the data and the time it was measured. Putting the data into a Microsoft Excel spreadsheet for further manipulation was the easiest way to sort the values, provided that the data are global and diffuse radiation is on a horizontal surface. Data regarding global radiation cover 27 consecutive years of measurements from 1964 to 1990 while data regarding diffuse radiation are available for only 3 years from 1990 to 1993.

Using Microsoft Excel's 'mid' function, we can separate the data into lines according to the position they occupy. Then, using 'AutoFilter Data' we can sequentially apply a particular template to a specific line to subtract the needed values. For example, mean monthly sums of global radiation on a horizontal surface can be used for global radiation values.

### 2.2. Solar radiation estimation using computer programming

A computer program has been developed that simulates solar radiation incidence on Earth. The initial conditions are discussed in the introduction. A complete listing of the Matlab code for the main program and subprograms is included in Appendix A. A description of the program structure is described in the following paragraphs. Figure 6 is a flow diagram of the computer program. All units for solar energy calculations are specified in SI.

www.manaraa.com

## 2.3. Extraterrestrial Radiation

Extraterrestrial radiation is radiation that would be incident on a horizontal plane on Earth with the absence of atmosphere. For engineering purposes, it is useful to know extraterrestrial radiation for comparison with measured and calculated values.

We need to know the extraterrestrial radiation value for comparison with the actual data listed in Appendix B. First of all, the value of radiation incident on a horizontal surface with respect to the atmosphere can never be higher than the extraterrestrial radiation value. If it is higher, it shows that the data is erroneous or that there is a mistake in the calculations.

Duffie & Beckman [7] recommend the following formula for calculating extraterrestrial radiation

$$H_o=(24\cdot 3600\cdot \frac{G_{sc}}{\pi})\cdot(1+0.033\cdot\cos\frac{360\times n}{365}\cdot\cos X\cdot\cos(\delta(n))\cdot\sin(\omega(n))+\left(\frac{\pi\times\omega(n)}{180}\right)\cdot \quad (2.1)$$
$$\cdot\sin X\cdot\sin(\delta(n))\ \frac{J}{m^2}$$

Where:

- n is the day of the year;
- X is the latitude;
- $\delta$ is the declination;
- $\omega$ is an hour angle;
- $G_{sc}$ is a solar constant.

www.manaraa.com

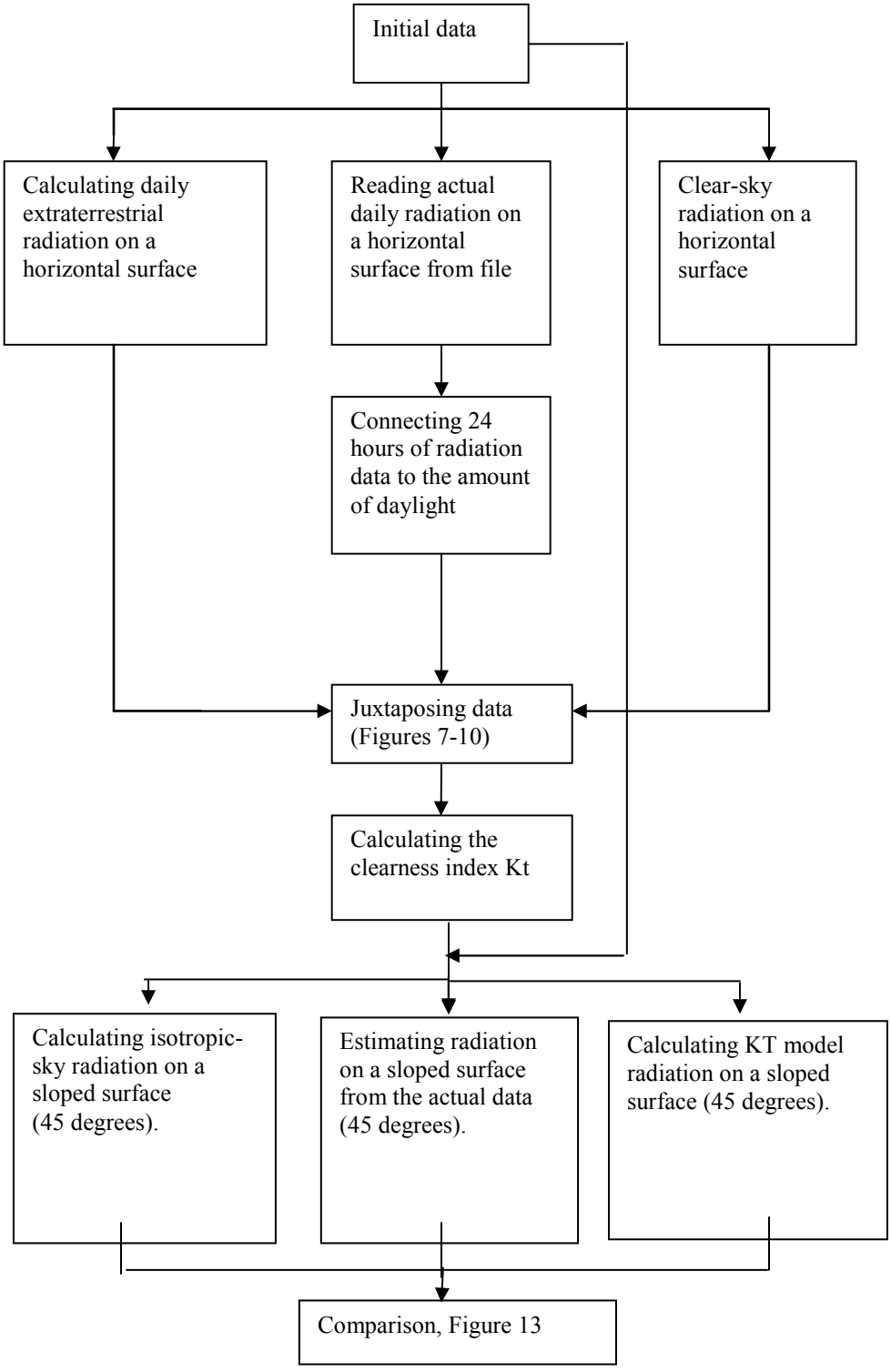


*Figure 6: Solar radiation program flow diagram*

www.manaraa.com

Note: $\left(\frac{\pi \times \omega(\mathrm{n})}{180}\right)$ converts degrees to radians. Matlab works with radians by default; therefore, simple functions were developed to convert degrees to radians and back again. These functions are listed in Appendix A ('rd', 'dr').

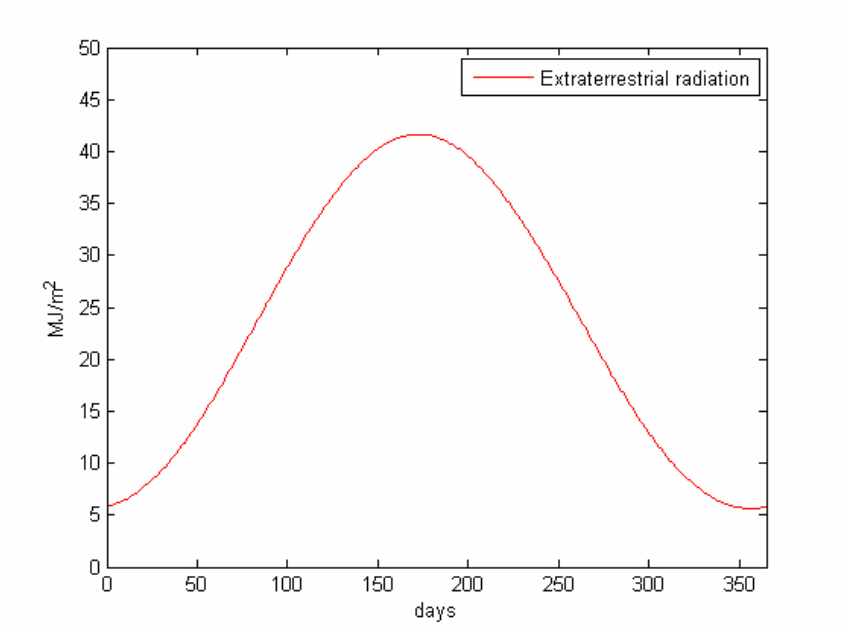


*Figure 7: Extraterrestrial radiation on a horizontal surface*

Figure 7 shows the change of extraterrestrial solar radiation in $\frac{MJ}{m^2}$ with respect to the number of days in a year. Figure 8 has been included here to show relationships between extraterrestrial radiation and actual data.

### 2.4. Clear-sky radiation

The clear-sky radiation model is a method of estimating clear-sky solar radiation with respect to the zenith angle and altitude for a standard atmosphere. This method distinguishes four different types of standard climates.

www.manaraa.com

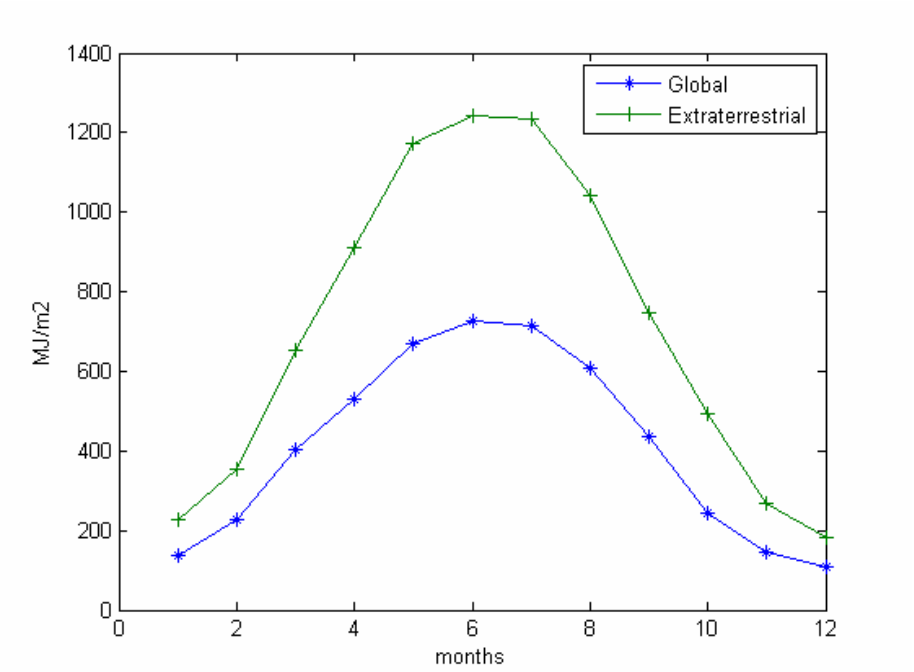


*Figure 8: Mean monthly sums of extraterrestrial and actual global radiation on a horizontal surface (Data covers 11 years from 1964 to 1991)*

Duffie & Beckman [7] named these types as: tropical, midlatitude, subarctic

Clear-sky beam radiation on a horizontal surface is

$$G_{cb} = G_{on} \cdot \tau_b \cdot \cos\theta_z \quad (2.2)$$

Where:

- $G_{on}$ is normal extraterrestrial radiation;
- $\tau_b$ is the atmospheric transmittance for beam radiation;
- $\cos\theta_z$ is a zenith angle.

The atmospheric transmittance for beam radiation is presented as

www.manaraa.com

$$\tau_b = a_0 \cdot r_0 + a_1 \cdot r \cdot \exp\left(\frac{-k}{\cos\theta_z} \cdot r_k\right) \quad (2.3)$$

Where:

- $r_0, r_1, r_k$ is the correction factors for climate types;
- $a_0, a_1, k$ is the functions of altitude;
- $\cos\theta_z$ is a zenith angle.

Due to the fact that $\tau_b$ is a function of $\theta_z$ , which changes with the time of day, the atmospheric transmittance must be computed for beam radiation for each daylight hour of each day of a year. Knowing the sunset hour angle $\omega_s$ is important since the sunset hour angle is the opposite of the sunrise hour angle. The sunset hour angle can be found from the following formula:

$$\cos\omega_s = \frac{\sin Lat \cdot \sin\delta}{\cos Lat \cdot \cos\delta} \quad (2.4)$$

or

$$\cos\omega_s = -\tan Lat \cdot \tan\delta \quad (2.5)$$

Where:

- Lat is a latitude;
- $\delta$ is the declination;

www.manaraa.com

The double value of this angle gives us the angle of sun movement from sunrise to sunset. It is also known that one hour equals $15^{\circ}$ of sun movement. Therefore, the number of daylight hours is:

$$N = \frac{2}{15} \cdot \left( -\tan Lat \cdot \tan \delta \right) \quad (2.6)$$

The values for $r_0$, $r_1$, $r_k$ are [7]:

$$\begin{aligned} r_0 &= 0.99 \\ r_1 &= 0.99 \\ r_k &= 1.01 \end{aligned} \quad (2.7)$$

The values for $a_0$, $a_1$, $k$ can be found as

$$\begin{aligned} a_0 &= 0.4237 - 0.00821 \cdot (6 - A)^2 \\ a_1 &= 0.4237 + 0.00595 \cdot (6.5 - A)^2 \\ k &= 0.2711 + 0.01858 \cdot (2.5 - A)^2 \end{aligned} \quad (2.8)$$

Where:

- A is an altitude , m.

The result of the calculation of the clear-sky model is shown in Figure 9. We can visualize the difference between 'ideal' extraterrestrial radiation on a horizontal surface and clear-sky model results, which are shown in Figure 10. Even though the clear-sky model can give a good approximation of global radiation values, it considerably underestimates global radiation (Figure 11). Switching to different types of climate did not improve the clear-sky model.

www.manaraa.com

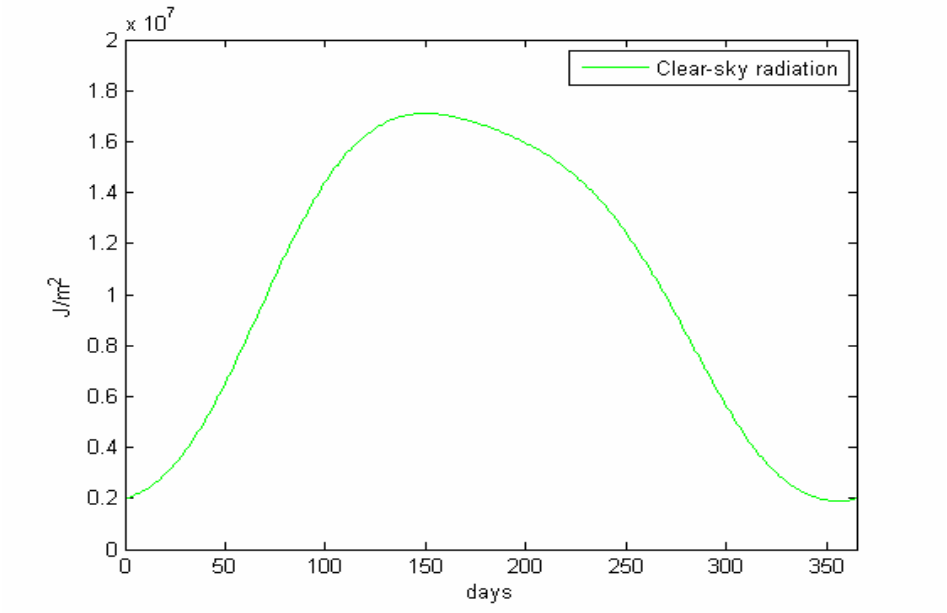


*Figure 9: Clear-sky radiation on a horizontal surface*

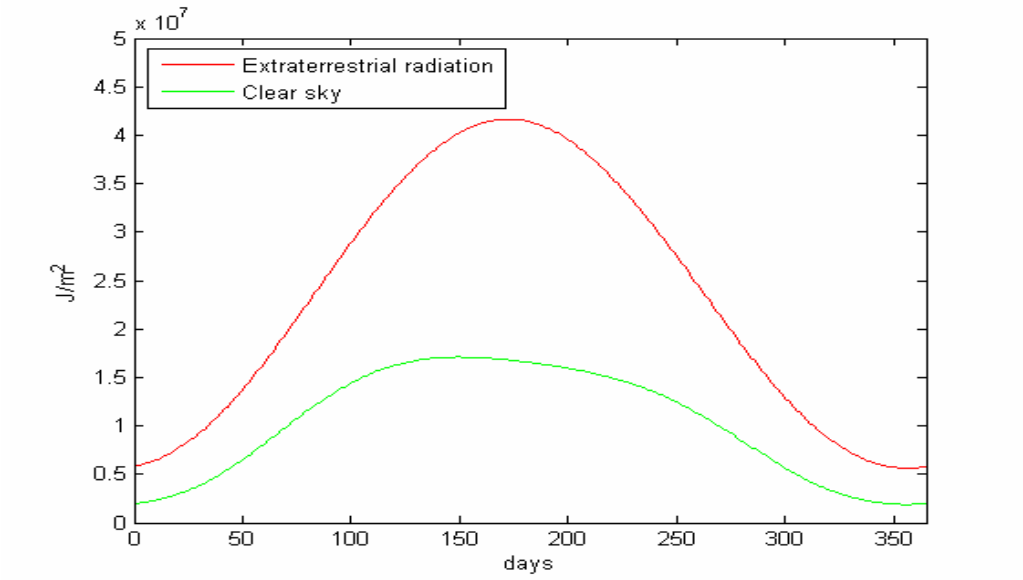


*Figure 10: Extraterrestrial and clear-sky radiation on a horizontal surface*

www.manaraa.com

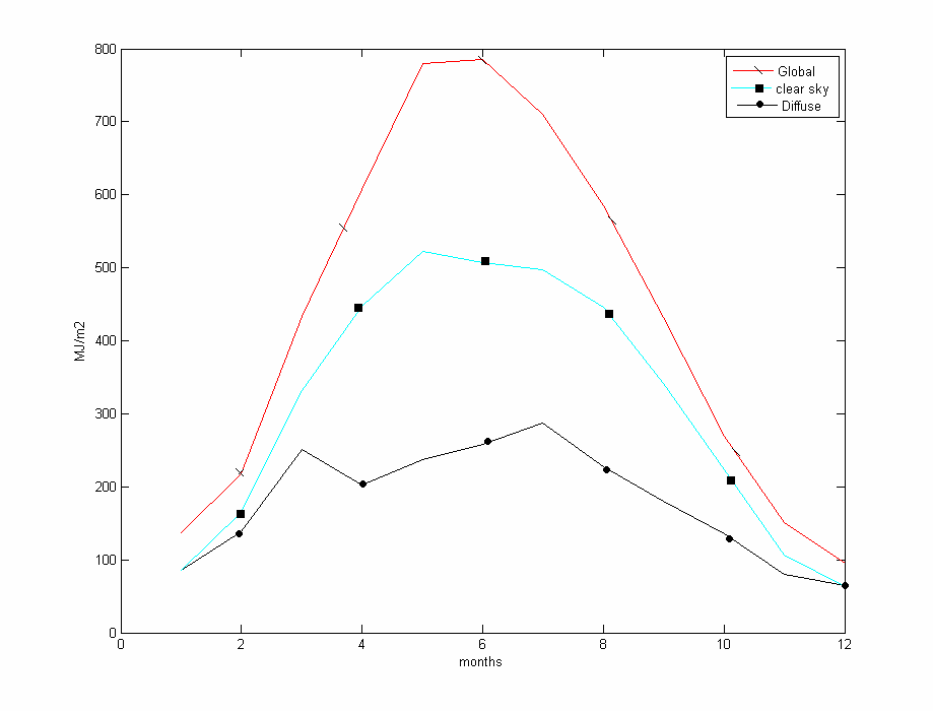


*Figure 11: Mean monthly sums of global, global clear-sky and diffuse radiations on a horizontal surface*

The clear-sky model is easy to understand but not precise enough for use in the estimation of radiation. Correction factors for four different types of climate do not take into account many factors that cause the scattering and absorption of beam radiation.

## 2.5. Radiation on a sloped surface

### 2.5.1. Isotropic sky

The isotropic-sky model implies that global radiation is isotropic, which means that that the sum of diffuse and beam radiation does not depend on the angle of attack. Diffuse radiation data retrieved from WRC [8] contain a lesser number of years than that

www.manaraa.com

of global radiation data. Hence, the Collares-Pereira and Rabal correlation for separation diffuse radiation from global radiation can provide more reliable values.

The Collares-Pereira and Rabal describes the values of beam and diffuse radiation as a function of $K_T$ [7].

$$\begin{aligned} &if\ K_T \le 0.17 && H_d = 0.99H \\ &if\ 0.17 < K_T \le 0.75 && H_d = H(1.188 - 2.27K_T + 9.473K_T^{\,2} - 21.865K_T^{\,3} + 14.648K_T^{\,4}) \\ &if\ 0.75 < K_T < 0.80 && H_d = (-0.54K_T + 0.632)H \\ &if\ \ K_T \ge 0.80 && H_d = (0.2)H \end{aligned} \qquad (2.11)$$

Figure 12 juxtaposes the results calculated with this correlation and actual data for the year 1992. The Average Clearness index $K_T$ was derived from 23 years of data for global radiation and extraterrestrial radiation on a horizontal surface.

### 2.5.2. KT method

KT stands for Klein and Theilacker, who developed a more detailed computation of the estimation of solar radiation. This method assumes that diffuse and ground reflected radiations are isotropic. This method shows better results than the isotropic-sky method.

www.manaraa.com

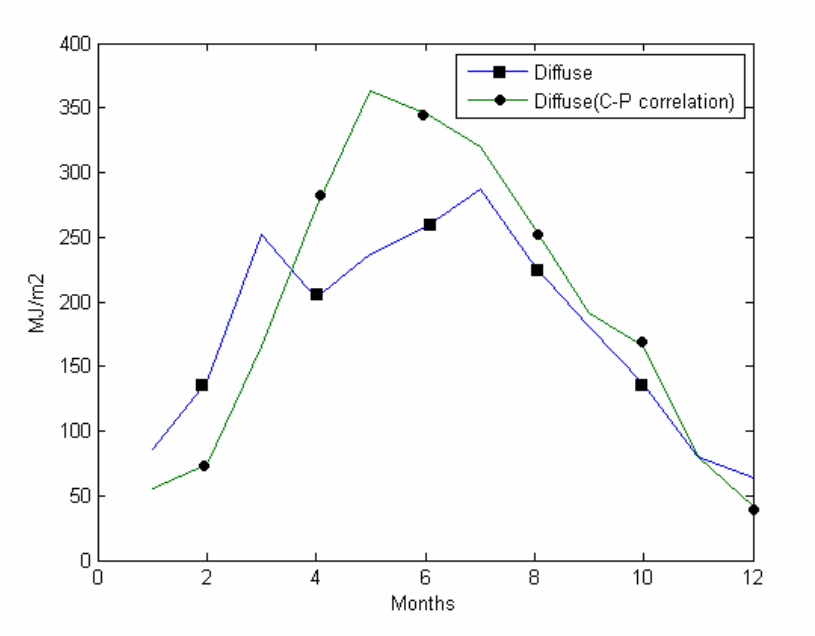


*Figure 12: Comparison of diffuse radiation calculated with the Collares-Pereira and Rabal correlation and actual data (1992).*

The monthly average radiation on a collector is

$$\bar{H}_{KT} = \bar{H} \cdot \bar{R} \qquad (2.12)$$

Where:

- $\bar{R}$ is the ratio of the total radiation on the tilted surface to the total radiation on a horizontal surface;
- $\bar{H}$ is the total radiation on a horizontal surface.

The ratio of a total radiation on the tilted surface to the total radiation on a horizontal surface can be found by:

www.manaraa.com

$$\bar{R} = \frac{\cos(Lat-\beta)}{d\cdot\cos(Lat)}\cdot\left[\left(a-\frac{\bar{H}_d}{\bar{H}}\right)\left(\sin\omega_s' - \omega_s'\cdot\cos\omega_s''\right)+\frac{b}{2}\cdot\left(\omega_s' + \sin\omega_s'\left(\cos\omega_s' - 2\cdot\cos\omega_s''\right)\right)\right]$$
$$+\frac{\bar{H}_d}{\bar{H}}\left(\frac{1+\beta}{2}\right)+\rho_g\left(\frac{1-\beta}{2}\right) \qquad (2.13)$$

$$\begin{aligned} a &= 0.409 + 0.5016\cdot\sin(\omega_s' - 60) \\ b &= 0.6609 - 0.4767\cdot\sin(\omega_s' - 60) \\ d &= \sin\omega_s' - \omega_s'\cdot\cos\omega_s' \\ \omega_s' &= \min\begin{bmatrix}\cos^{-1}(-\tan Lat\cdot\tan\delta) \\ \cos^{-1}(-\tan(Lat-\beta)\cdot\tan\delta)\end{bmatrix} \\ \omega_s'' &= \cos^{-1}(-\tan(Lat-\beta)\cdot\tan\delta) \end{aligned} \qquad (2.14)$$

Where:

- $\rho_g$ is the ground reflectance;
- Lat is the Latitude;
- $\bar{H}$ is the total radiation on a horizontal surface;
- $\bar{H}_d$ is the diffuse radiation on a horizontal surface;
- $\beta$ is the surface slope;
- $\omega_s'$ is the hourly angle.

Figure 13 shows the comparison among radiation values obtained from actual data, the KT mode, and the isotropic-sky model. We can see that both KT and clear-sky models show a plausible approximation of solar radiation on a sloped surface.

www.manaraa.com

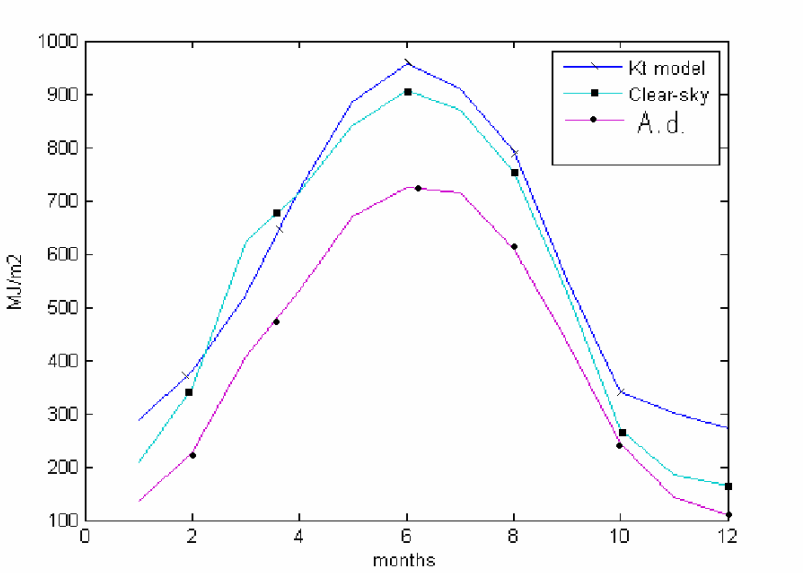


*Figure 13: Comparison of actual radiation on a horizontal surface with isotropic-sky and KT model radiation on a sloped surface (45 degrees)*

## 2.6. Optimal slope

The optimal slope is a slope that allows the surface to receive the maximum amount of incident radiation. Using the Matlab optimization function 'fminsearch' we can find the optimal slope angle for receiving the maximum amount of solar radiation on a sloped surface. We assume that the surface azimuth angle is zero, which means that the collector should be placed along the north-south axis.

Figure 14 graphically shows that change with respect to the time of the year. As we can see for the coldest month, the optimal slope is very high (up to 80 degrees) since the latitude of the location is high. This fact corresponds to some researchers' recommendations [7] for installing solar collectors on walls as a way to improve solar energy absorption at wintertime and eliminating precipitation influence on performance.

www.manaraa.com

Empirical values for the optimal slope are latitude value plus 15 degrees in the winter and latitude value minus 15 degrees in the summer [9]. The effect of the slope on the absorption of solar radiation is discussed below.

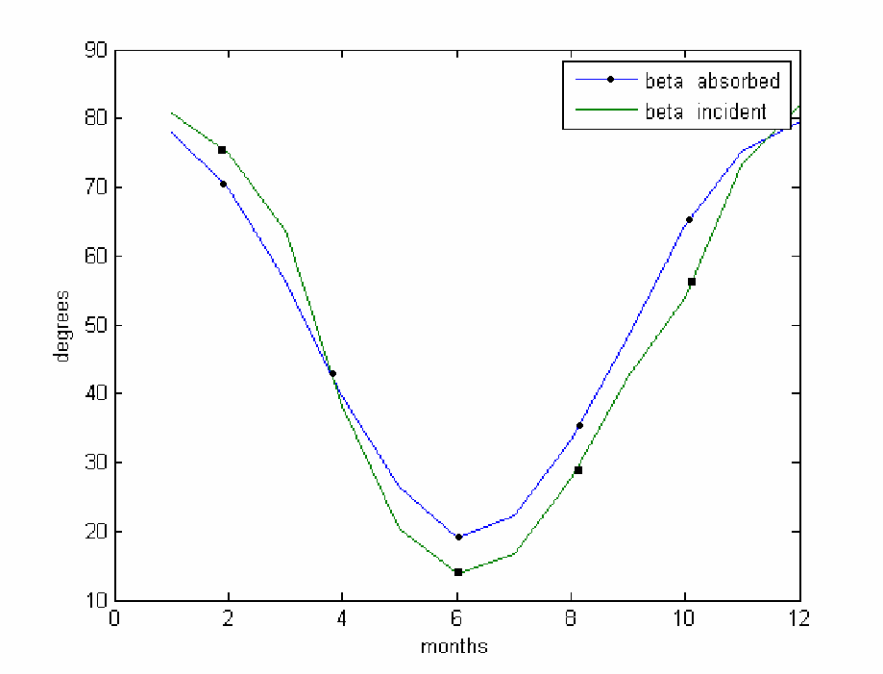


*Figure 14: Comparison of optimal slopes for maximum incident radiation and maximum absorbed radiation (azimuth angle is zero).*

## 2.7. Absorbed radiation

Absorbed radiation is a function of plate and cover characteristics and the incident angle of radiation. Since glass is the most common material for cover, all characteristics of cover are assumed to be independent of wavelength, which is a good assumption for glass. Glass with low iron content ('water white') is a good material for cover since it has high transmittance.

For application as solar collectors it is convenient to use a transmittance absorptance product $(\tau\alpha)$ for the calculation of the amount of radiation that is

www.manaraa.com

transmitted to the absorber plate. The transmittance absorptance product $(\tau\alpha)$ is a figure of merit that tells us how much energy passing through the cover is reflected by the absorber plate and reflected back by the cover.

$$(\tau\alpha) = \frac{\tau\alpha}{1-(1-\alpha)\rho_d} \quad (2.15)$$

Where:

- $\tau$ is the transmittance of the cover;
- $\alpha$ is the absorptance of the cover;
- $\rho_d$, is the reflectance of the absorber plate for diffuse radiation.

Reflectance of the absorber plate contributes a great deal to the overall performance of a solar collector. The absorber plates of modern solar collectors have two major characteristics: high absorptance of solar radiation and low emmitence in a long-wave spectrum (i.e., selective surfaces).

A Matlab code for solar radiation estimation (Appendix A) includes transmittance absorptance product $(\tau\alpha)$ calculations (Figure 15). Assuming unpolarized radiation, we can calculate perpendicular and parallel components of unpolarized radiation to obtain the transmittance absorptance product.

$$r_{\perp} = \frac{\sin^2(\theta_2-\theta_1)}{\sin^2(\theta_2+\theta_1)}$$
$$r_{\square} = \frac{\tan^2(\theta_2-\theta_1)}{\tan^2(\theta_2+\theta_1)} \quad (2.16)$$
$$\theta_2 = \sin^{-1}\frac{\sin\theta_1}{n}$$

Where:

www.manaraa.com

- $r_{\perp}$ ,is the perpendicular component of incident radiation;
- $r_{\parallel}$ is the parallel component of incident radiation;
- $\theta_1$ is the angle of incident radiation;
- $\theta_2$ is the refraction angle of incident radiation.

The average transmittance of glass cover is the average transmittance of two components:

$$\tau_r = \frac{1}{2}\left(\frac{1-r_{\parallel}}{1+r_{\parallel}} + \frac{1-r_{\perp}}{1+r_{\perp}}\right) \quad (2.17)$$

Where 'r' stands for refraction losses;

$$\tau_a = \exp\left[-\frac{KL}{\cos\theta_2}\right] \quad (2.18)$$

Where:

- K is the extinction coefficient assumed to be 4 $m^{-1}$ for low iron glass;
- L is the glass thickness, m;
- The subscript 'a' stands for absorption losses.

Overall transmittance of a single cover can be found as:

$$\tau \cong \tau_a \tau_r \quad (2.19)$$

Absorptance of a solar collector cover can be found as:

$$\alpha = 1 - \tau_a \quad (2.20)$$

Reflectance of a single cover can be found as:

$$\rho = \tau_a - \tau \quad (2.21)$$

www.manaraa.com

Important assumptions were made for the calculation of beam radiation $(\tau\alpha)$. The function of incident angle $(\tau\alpha)$ varies diurnally; therefore, complex calculations are required. However, using an incidence angle that occurs 2.5 hours after the solar noon on an average day of the month, we can calculate $(\tau\alpha)$ close to a real value of $(\tau\alpha)$ [7]. This empirical assumption is valid for space heating applications and does not give acceptable results for other applications due to its narrow specialization of the application. Transmittance absorptance products for diffuse radiation and ground reflected radiation are the functions of the collector's slope and do not change with time. The isotropic-sky model was used to take into account transmittance absorptance products.

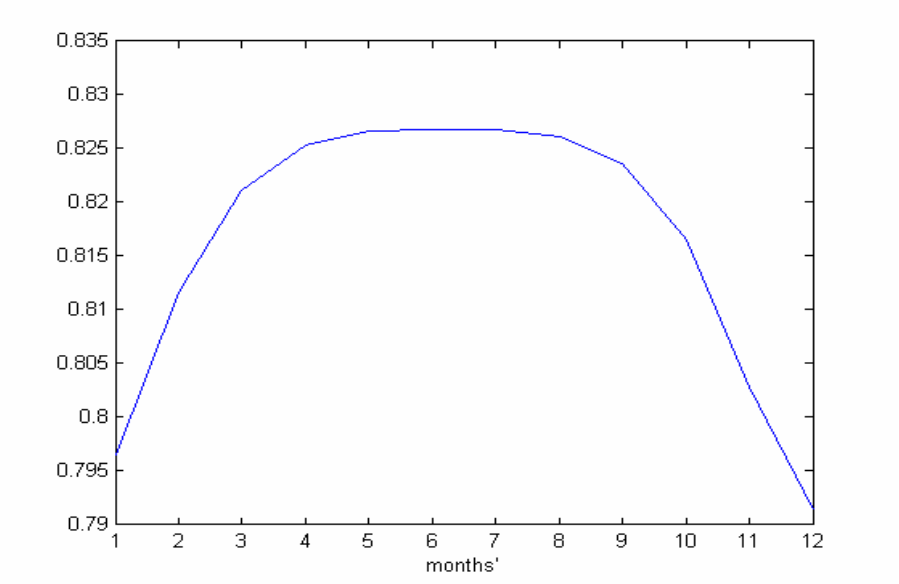


*Figure 15: Average transmittance absorptance product fluctuation.*

The following formula differs from the original formula (2.9) with transmittance-absorptance products.

www.manaraa.com

$$\overline{S} = \overline{H}_b \overline{R}_b (\overline{\tau\alpha})_b + \overline{H}_d (\overline{\tau\alpha})_d \left(\frac{1+\beta}{2}\right) + \overline{H}\rho_g (\overline{\tau\alpha})_g \left(\frac{1-\beta}{2}\right) \quad (2.22)$$

Note: subscripts b, d and g stand for beam diffuse and ground.

Where:

- Sbar daily is the absorbed radiation on a sloped surface corresponding to the optimal angle for incident radiation, MJ/m2;
- Global daily and diffuse daily are the average vales of radiation on a horizontal surface, MJ/m2;
- Sbar daily fixed is the absorbed radiation corresponding to a fixed angle of 70 degrees, MJ/m2;
- Sbar optimum is the absorbed radiation corresponding to the optimal angle for absorbed radiation, MJ/m2.

This model was used in the Matlab simulation as a function 'absorbed'. The result of this computation is shown in Figure 16.

Figure 17 is a replica of Figure 16 and represents the relationship between daily radiation and the number of sunshine hours. The lines are concaved up since the number of hours of sunshine is greater in the summer. Conversion to watts is made as a function of 'absorbed' (Appendix A).

The separation of diffuse radiation from beam radiation has been described previously (the Collares-Pereira and Rabal correlation). Diffuse radiation is assumed to be constant all day. In the same manner, beam radiation is assumed to be incident on a surface only during bright sunshine hours. We need to know this information in order to use the concept of utilizability.

www.manaraa.com

## 2.8. Utilizability

The amount of energy absorbed is as important as the period when this energy is being absorbed. Being a function of the loss coefficient, the useful gain must be greater than losses to the environment. Therefore, there is a minimum value of absorbed radiation that cannot be reached in order to avoid losing energy that is stored. This is called a "critical radiation level" or "threshold radiation." This level depends on the transmittance-absorptance product and overall loss coefficient.

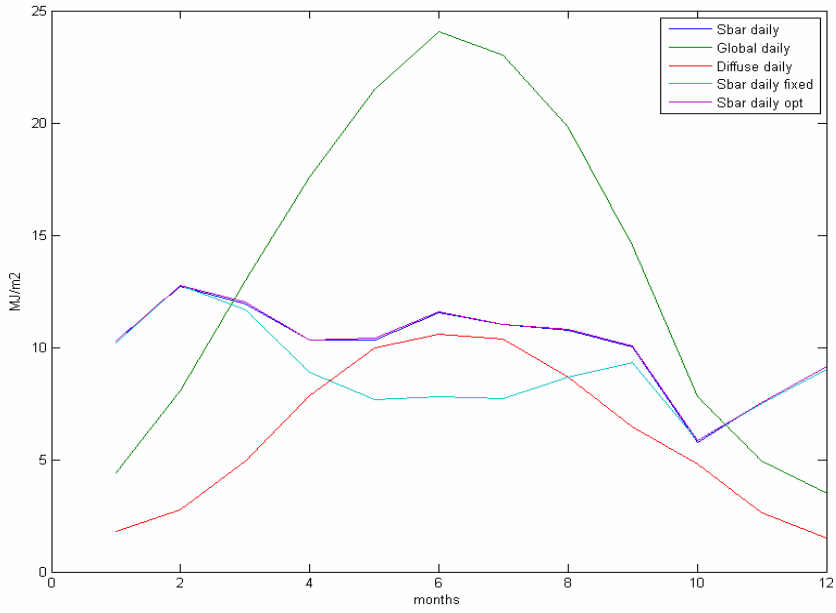


*Figure 16: Comparison of daily radiation on a horizontal surface to absorbed radiation on sloped surfaces with different angles.*

This level can be found by:

$$H_{cr} = \frac{U_l(T_p - T_a)}{(\tau\alpha)} \quad (2.23)$$

or

www.manaraa.com

$$\overline{S_{cr}} = U_l(T_p - T_a) \quad (2.24)$$

Where:

- $H_{cr}$ is the critical radiation level, MJ/m2;
- $U_l$ is the overall loss coefficient, W/m C;
- $(\tau\alpha)$ is the transmittance-absorptance product;
- $T_p$ is the plate temperature, C;
- $T_a$ is the ambient temperature, C;
- $\overline{S_{cr}}$ is the critical absorbed radiation level, MJ/m2.

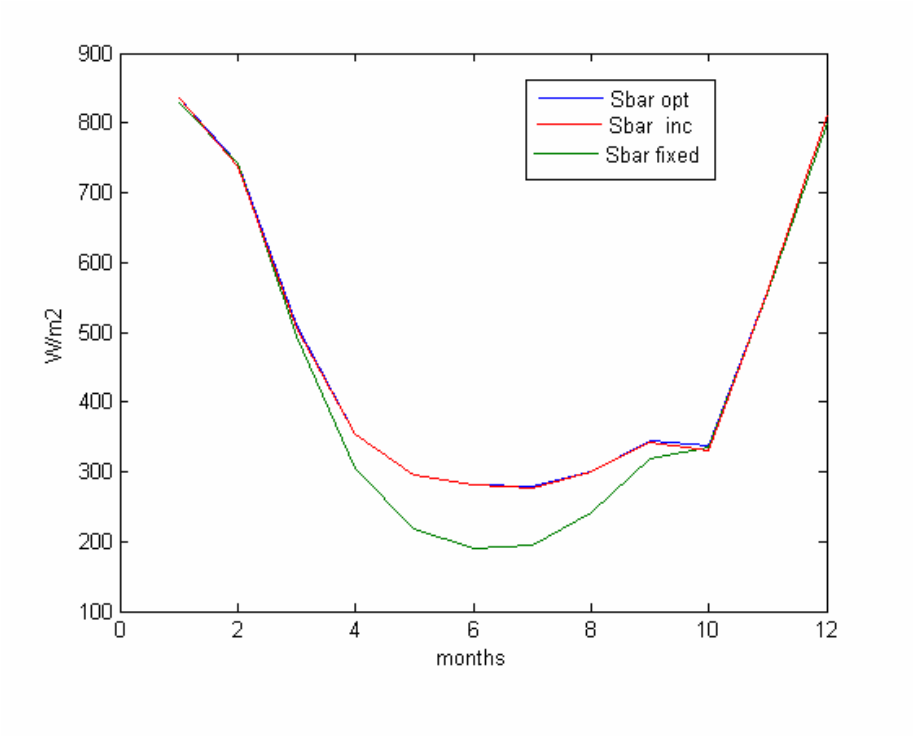


*Figure 17: Comparison of values of absorbed radiation on sloped surfaces with different angles (W/m2).*

www.manaraa.com

Due to the lack of actual radiation and ambient temperature values we cannot use this concept and must rely on a control system that will shut pumps down when the solar radiation level is less then its losses. However, in the computer program this concept is a condition that checks if the outflow temperature from the collector is lower than the inflow temperature. In that case, the system considers the solar collector as offline.

www.manaraa.com

## 3. SOLAR COLLECTORS

Usually the category name of a solar collector is determined by its working fluid (water, air). Several types of flat-type solar collectors are available for use in residential buildings. General categories are:

- Unglazed flat-type liquid-type solar collectors;
- Evacuated tube solar collectors;
- Glazed flat-type liquid-type solar collectors;
- Air-type collectors.

Unglazed flat-type liquid-type solar collectors are primarily used for the heating of swimming pools since they cannot provide high water temperatures in severe climates.

Glazed flat-type liquid-type solar collectors are the most common type of solar collectors available. They allow solar energy to be used in severe climates since their glass covers can significantly reduce convective heat losses.

Air-type collectors have less efficiency compared to liquid-type collectors, but they have fewer problems with operation and maintenance since air is a less aggressive substance than water or other liquids.

In addition, there are other types of solar collectors, such as evacuated tube solar collectors and parabolic trough solar collectors.

Evacuated tube solar technology has eliminated conductive heat losses. The efficiency of evacuated tube solar collectors is very high. However, due to their fragility and difficulties with snow removal from space between the tubes, the evacuated tube solar collectors are not considered a viable option for this project. Parabolic trough solar

www.manaraa.com

collectors are a technology that allows the concentration of solar energy incident on a reflective parabolic surface to a certain point such that the concentrated energy can be converted to heat. This technology is still too expensive and cumbersome for use in residential heating.

The residential house previously described in the introduction has an orientation such that the two slopes of the roof face west and east. This complicates placing solar collectors since the optimum direction of the solar collector slope in most cases is south. In order to avoid losing solar energy at sunset and sunrise and placing solar collectors on the roof, the orientation of the house should be constructed along the west to east axis. This means that the surface azimuth angle is zero. Since the project has not yet been built, the orientation can be easily modified.

The flat-type liquid-type solar collector is used as the basic unit in this thesis. The differences among flat-type solar collectors are subtle; therefore, a common type will cover all the advantages and disadvantages of this type of device. The choice of solar collector was made according to the specifications provided by the manufacturer.

The Canadian manufacturers of the model G32-P series solar collectors (Figure 18), Thermal Systems LTD [10] have a great deal of information on performance of their products. They have been certified by the Solar Rating & Certification Corporation and have a high degree of efficiency [4]. A full description of this solar collector is given in Appendix C. The major advantage that differentiates this solar collector from the average solar collector is the "Solarstrips $^{TM}$ " tubes, which are embedded in the absorber plate and which allow thermal resistance between the absorber and the tube walls to be disregarded.

www.manaraa.com

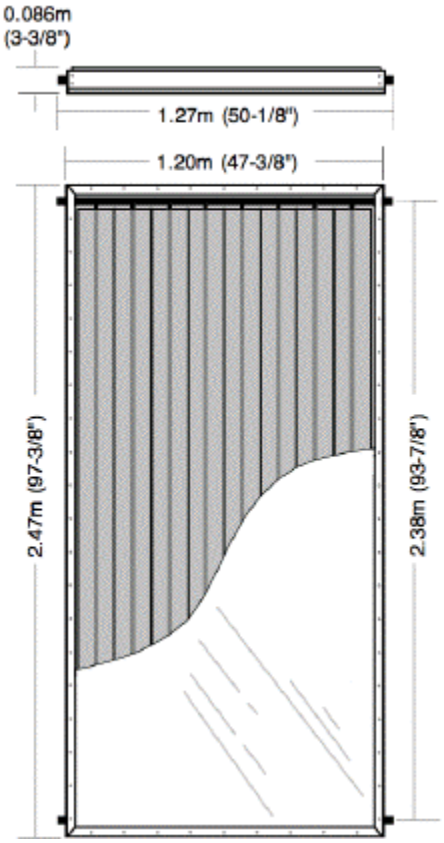


*Figure 18: G series solar collector, Thermal systems LTD.*

### 3.1. Energy balance in a flat-type solar collector

Energy balance in a single covered collector is presented in Figure 19.

$$Q_u = A_c\left[S - U_L(T_{pm} - T_a)\right] \quad (3.1)$$

Where:

- $Q_u$ is useful gain, MJ/m2;
- $A_c$ is the collector area, $m^2$;
- $S$ is absorbed energy, W/m2;

www.manaraa.com

- $U_L$ is the overall loss coefficient, W/m2-C;
- $T_{pm}, T_a$ is the plate mean temperature and ambient temperature, C.

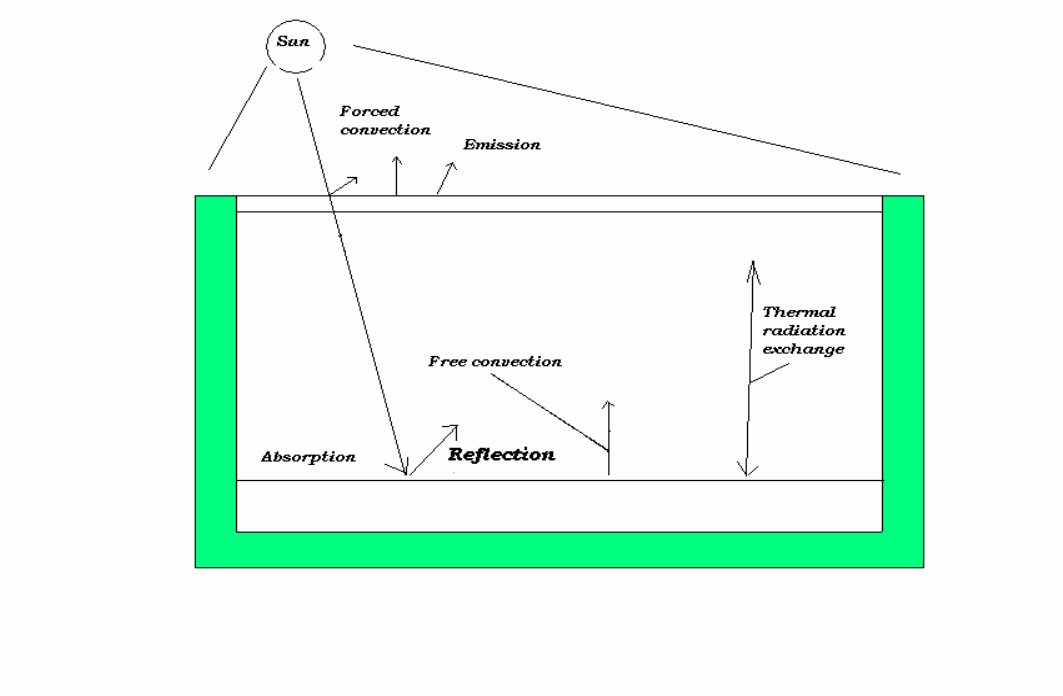


*Figure 19: Heat transfer processes in a single glass solar collector.*

### 3.1.1. Assumptions

The following assumptions are often used in solar collector simulations:

- The properties of all materials are constant;
- The covers are opaque to infrared radiation;
- 1D Heat flux is [experienced] through a cover;
- The sky is a black body with an equivalent sky temperature;
- The dust effect on the solar collector's performance is negligible.

www.manaraa.com

### 3.2. Overall loss coefficient

The overall loss coefficient is a key value in the study of the performance of a solar collector. It consists of several components, namely:

- The top loss coefficient;
- The edge loss coefficient;
- The back loss coefficient.

The top loss coefficient has two parts: the losses from plate to cover and from cover to the ambient or wind convection coefficient. Loss from cover to plate can be found as a function of the Rayleigh number and slope. Figure 20 shows the iteration process in Matlab function 'Ul' (Appendix A).

$$
\begin{aligned}
&Nu = 1 + 1.44\left[1 - \frac{1708}{Ra\cos\beta}\right]^{+}\left(1 - \frac{\sin(1.8\beta)1708}{Ra\cos\beta}\right) + \left[\left\{\frac{Ra\cos\beta}{5830}\right\}^{1/3} - 1\right]^{+} \\
&Ra = \frac{gB\Delta T}{\upsilon\alpha} \\
&for \qquad 75 \le \beta \le 90 \\
&Nu = \left[1, 0.288\left(\frac{\sin\beta Ra}{A}\right)^{1/4}, 0.039(\sin\beta Ra)^{1/3}\right]_{\max}
\end{aligned}
\tag{3.2}
$$

Where:

- Nu is a Nuselt number;
- Ra is a Rayleigh number;
- $\beta$ is an inclination;
- B , is a reciprocal of temperature (assuming air is Ideal Gas);
- $\upsilon\alpha$ is viscosity and thermal diffusivity;

www.manaraa.com

- A is the ratio of the length of the collector to space between the absorber and the cover.

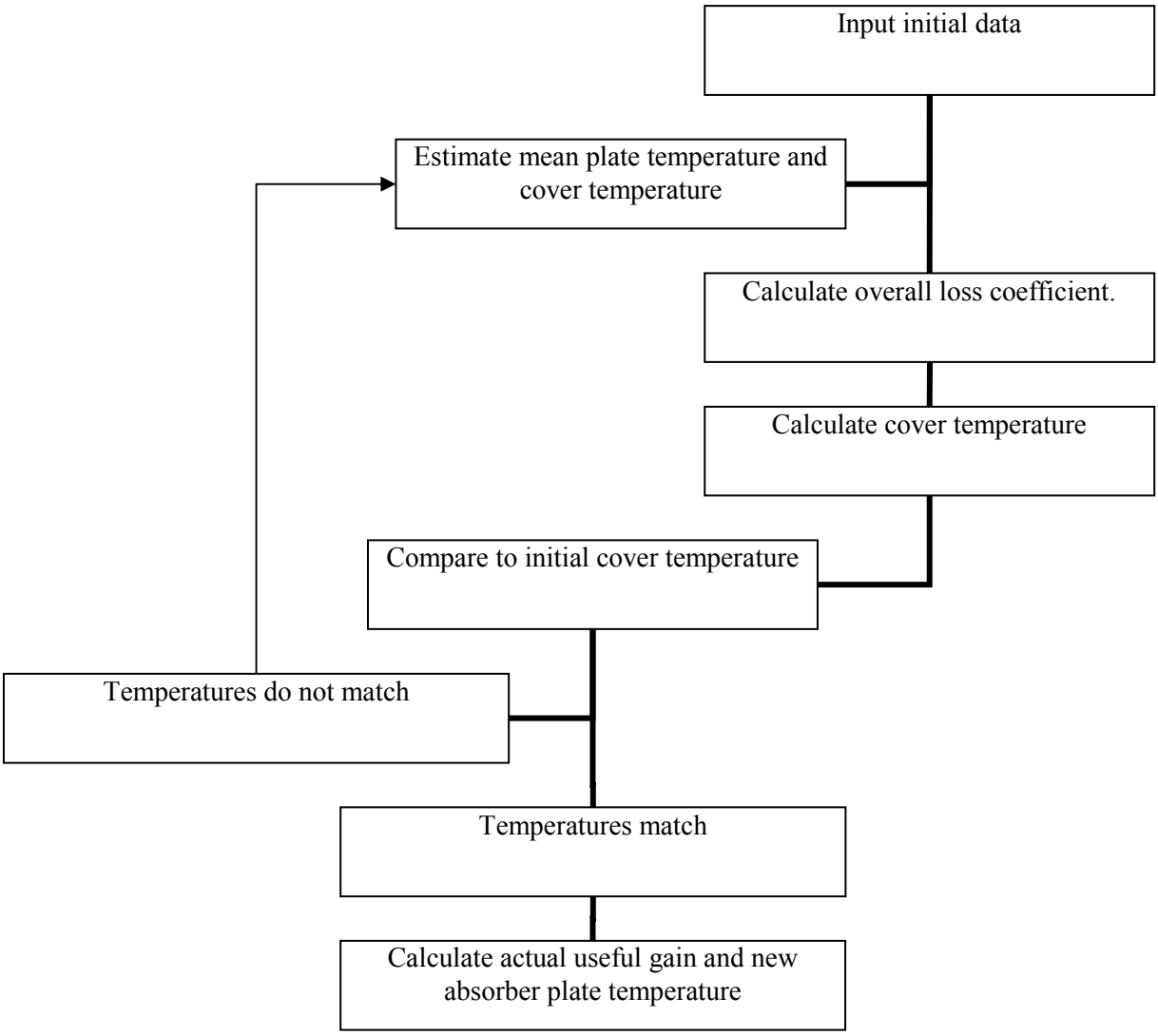


*Figure 20: Flow chart of solar collector simulation.*

www.manaraa.com

Knowing the Nuselt number, the heat transfer coefficient from plate to glass becomes:

$$h_c = Nu\frac{K}{L} \qquad (3.3)$$

Where:

- K is the thermal conductivity of air estimated at film temperature W/m K;
- L is the space between cover and absorber, m.

The wind convection coefficient for the calculation of convection heat transfer on the cover of a flat collector mounted on a house can be found by using this empirical correlation [7]:

$$h_w = 2.8 + 3V \quad (3.4)$$

Where:

- $h_w$, wind loss coefficient, W/m C;
- V, Wind speed, m/s.

The Radiation coefficient form plate to glass is:

$$h_r = \varepsilon_{eff}\delta\frac{Tp^4 - Tg^4}{Tp - Tg} \quad (3.5)$$

Where:

- Tp and Tg are the glass and plate temperatures, K;
- $\delta$ is the Stefan-Boltzmann constant, $W\cdot m^{-2}\cdot K^{-4}$;
- $\varepsilon_{eff}$ is the effective emissivity of the plate-glazing system.

$$\varepsilon_{eff} = \left[\frac{1}{\varepsilon_p} + \frac{1}{\varepsilon_g} - 1\right]^{-1} \quad (3.6)$$

Where $\varepsilon_p$ and $\varepsilon_g$ are plate and glass emmisivities.

www.manaraa.com

The radiation coefficient from the glass to the ambient can be estimated from the sky temperature ( $T_a$ , $^{\circ}C$ ):

$$T_{sky}=T_a-6 \qquad (3.7)$$

$$h_{r-sky} = \varepsilon_g \delta \frac{Tg^4 - Ts^4}{Tg - Ta} \qquad (3.8)$$

Where:

- Ts, Tg are the sky and glass temperatures, K;
- $\varepsilon_g \delta$ ,is the emissivity of the glass and Stefan-Boltzmann coefficient; $T_a$ is the ambient temperature, K.

Combining the top loss coefficient of all components becomes:

$$U_t = \left[ \frac{1}{h_c + h_r} + \frac{1}{h_w + h_{r-sky}} \right]^{-1} \qquad (3.9)$$

The back loss coefficient can be found by:

$$U_b = \frac{k}{L} \qquad (3.10)$$

Where:

- k is the insulation thermal conductivity, W/m C;
- L is the insulation thickness, m.

Edge loss coefficient

$$U_e = U_b \frac{Ae}{Ac} \qquad (3.11)$$

Where:

- Ae is the edge area, m;

www.manaraa.com

- Ac is the collector area, m.

Finally $U_l$ can be found as a sum of previously discussed terms:

$$U_l = U_e + U_b + U_t \qquad (3.12)$$

It is convenient to find collector heat removal and collector efficiency factors. Collector efficiency can be found as [9]:

$$F' = \frac{1/U_L}{W\left[\frac{1}{U_L\left[D+(W-D)F\right]}+\frac{1}{C_b}+\frac{1}{\pi D_i h_{fi}}\right]}$$

$$F = \frac{\tanh[m(W-D)/2]}{[m(W-D)/2]} \qquad (3.13)$$

$$m = \sqrt{\frac{U_L}{k\delta}}$$

$$C_b = \frac{kb}{\gamma}$$

Where:

- W is the spacing among tubes, m;
- $U_L$ is the overall loss coefficient, W/m C;
- $F'$ is the collector efficiency;
- F is the standard fin efficiency for straight fins with a rectangular profile;
- D is the tube diameter, m;
- $k$ is the thermal conductivity of the bond between the tube and the absorber plate ,W/m C;

www.manaraa.com

- $\delta$ is the thickness of the absorber plate, m;
- $C_b$ is the bond conductance, which is a function of bond conductivity, width, and average thickness (since in this particular solar collector tubes are metallurgically bonded into the absorber plate, $C_b$ is very big; therefore, it can be disregarded);
- $h_{fi}$ is the heat transfer coefficient inside of tubes, W/m C.

### 3.3 The heat transfer coefficient

The heat transfer coefficient inside of the solar collector tubes can be approximated as a heat transfer coefficient with uniform heating of the tube. In other words, heat flux to the fluid is an overall constant of the tube surface [11]. Calculating the heat transfer for propylene glycol is not convenient since the thermodynamic properties of propylene glycol are not widely spread. There is some information on material properties at certain temperatures and concentration, but this information is not enough for curve fitting for use as a reference. Consequently, the thermodynamic properties of propylene glycol are assumed to be constant (Table 4). On the other hand, the thermodynamic properties of air and water are widely spread and were used as a way to approximate the simulation to real conditions [12, 13].

The heat transfer coefficient in solar collector tubes can be found by:

$$\begin{bmatrix} 0.7 \le \mathrm{Pr} \le 160 \\ \mathrm{Re}_D \ge 10000 \\ L/D \ge 10 \end{bmatrix}$$

$$f = (0.79\ln(\mathrm{Re}_D) - 1.64)^{-2}$$

www.manaraa.com

$$Nu_D = \frac{(f/8)(\mathrm{Re}_D - 1000)\,\mathrm{Pr}}{1 + 12.7(f/8)^{0.5}(\mathrm{Pr}^{2/3} - 1)}$$

$$h_{fi} = Nu_D \frac{k}{D} \qquad (3.14)$$

Where:

- F is the Darcy friction coefficient;
- Pr, Nu, Re are the Prandtl, Nuselt and Reynolds numbers;
- $h_{fi}$ is the heat transfer coefficient, W/m C.

Note: subscript d stands for hydraulic diameter which is used to calculate the Re number.

www.manaraa.com

# 4. SOLAR HEATING SYSTEM SIMULATION

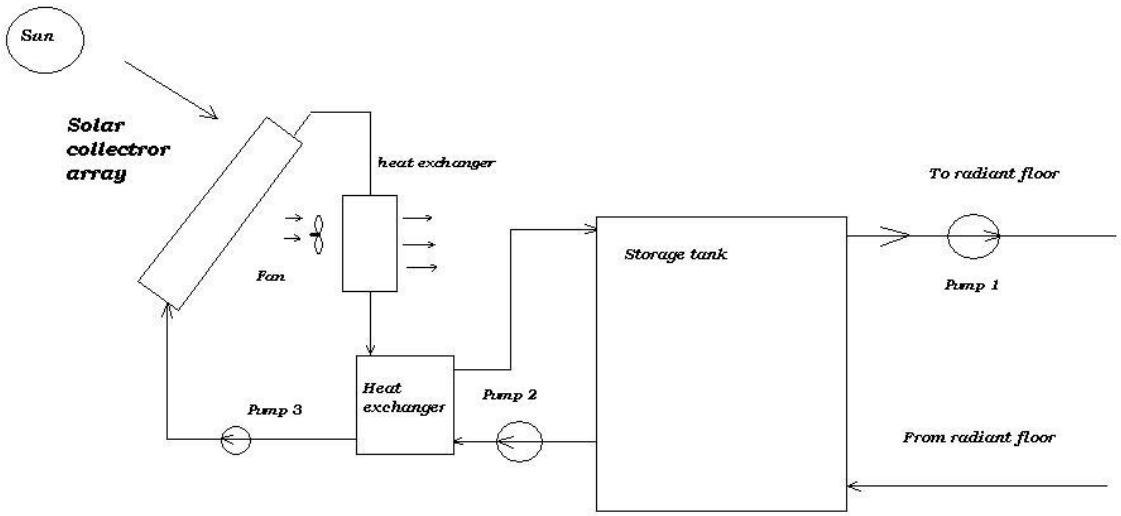


*Figure 21: Solar space heating system.*

Figure 21 shows the schematic diagram of the solar heating system of the residential building that is simulated in this study. This system has a typical configuration and showed good results in a number of studies [7].

The roof dimensions allow us to place up to 24 solar collectors (72 meters of solar collectors) in two rows. Common practice is to use a mixed connection of solar collectors to improve solar heating system performance [9]. We can use panels of 4 collectors connected in parallel and 6 panels connected in a series (Appendix C: Typical double tier solar collector array). The slope of the collectors is assumed to be fixed at 70 degrees for all months since changing the slope requires some kind of control system which the small increase of absorbed radiation cannot justify.

www.manaraa.com

## 4.1. Heat exchangers

A water/glycol heat exchanger has been chosen as recommended by the manufacturer. Following the manufacturer selection guide, the area of the heat exchanger is found (a worksheet can be found in Appendix C). The heat transfer load can be found as: 72 meters of solar collector multiplied by 850 $W/m^2$ (maximum absorbed radiation: Figure 17), which provides 205 MBtu/hr. The shell side fluid is propylene glycol. The rest of the computation is in Appendix C. The operation cost is estimated separately in the program (Appendix A). An air glycol heat exchanger is a typical air-type heat exchanger with common parameters ( Table 3).

*Table 3: Heat exchanger characteristics*

| Type / Property | Finned-tube heat exchanger | Shell-tube heat exchanger |
|---|---|---|
| U ($W/m^2K$) | 200 | 216 |
| Working fluids<br>-shell side<br>-tube side | Air<br>propylene glycol | Propylene glycol<br>Water |
| Area, m | 8 | 8 |

## 4.2. Thermal energy storage

There are numerous methods of storing thermal energy. The thermal capacity of a solar collector should be as small as possible since this energy will be lost to the environment. Therefore, we have to store thermal energy outside of the collector. The effectiveness and feasibility of these methods depend on the object's designation and cost.

www.manaraa.com

In this thesis we use flat-plate-type liquid-type solar collectors coupled with a radiant heating system which is embedded within a concrete slab. The slab is 4 inches thick, and does not have enough storage capacity to store and distribute the required amount of thermal energy for an adequate period. Hence, additional storage is required to provide backup at night and on cloudy days.

Liquid-type solar collectors in cold climates require the use of antifreeze. In the same manner, the use of water in a radiant heating system is a common practice. Therefore, the heating system must have a heat exchanger to transfer energy from antifreeze to water.

*Table 4: Propylene glycol thermodynamic properties [14]*

| Properties | Value | Notes |
|---|---|---|
| Boiling point | 187 | °C (lit.) |
| Melting point | −60 | °C (lit.) |
| Density | 1.036 | g/mL at 25 °C(lit.) |
| Price | 16 | $/gallon. |
| Specific heat | 3.806 | kcal/(kg-C) (50% concentration) |
| Thermal Conductivity | 0.34 | W/m-K 50% H2O @90°C |
| Viscosity | 3.1 | g/m s |

The most common, simple, and sensible thermal storage is a water tank. A multi-tank system configuration provides as much energy storage as a single storage tank of

www.manaraa.com

twice the volume [15]. In addition, a multi-tank system configuration can be presented as single tank storage of twice the volume.

Any water tank with heat inflow and outflow experiences stratification to some degree [16]. A stratified tank can be represented by several mathematical models. All of them can be classified as a *multimode* model. Even a well-mixed storage tank model can be called a *multimode* model since it implies a one-node tank model. Experimental data does not verify improvement of the mathematical model with the increase of the numbers of nodes since high stratification in a small capacity storage tank is unlikely [7]. Hence, a two-node model has been used in the simulation.

Hot water from a solar collector does not change the tank temperature immediately. The time after which heat collected by the solar collector reaches the bottom of the storage tank and changes the performance of the system is called a *turnover period*. Collected heat from the solar collector is equal to the heat required to raise the temperature of the storage from $T_{si}$ to $T_{so}$.

$$Q_t = \dot{m}_w C_w (T_{fo} - T_{fi}) t_s = M_s C_w (T_{so} - T_{si}) \qquad (4.1)$$

Assuming a two-node tank we can say $T_{fo} = T_{so}; T_{fi} = T_{si}$. Hence, the turnover period can be calculated as:

$$t_t = \frac{\dot{m}_w C_w}{M_s C_w} \qquad (4.2)$$

Where:

- $\dot{m}_w$ is the water flow rate, kg/s;
- $C_w$ is the specific heat of water, $\frac{\text{J}}{\text{kg K}}$;

www.manaraa.com

- $M_s$ is the storage capacity, kg;
- $T_{fo}$, is the temperature of the water leaving the water/glycol heat exchanger, C;
- $T_{fi}$ is the temperature of the water entering the water/glycol heat exchanger, C;
- $T_{so}$ is the temperature of the first node, C;
- $T_{si}$ is ,the temperature of the second node, C.

The new water temperature after a turnover is:

$$T_{so} = T_{si} + \frac{Q_u}{\dot{m}_s C_s} \qquad (4.3)$$

Where:

- $T_{so}$ is the storage outlet temperature, C;
- $T_{si}$ is the storage inlet temperature, C;
- $Q_u$ is the useful gain, W;
- $\dot{m}_s C_s$ are the water parameters.

## 4.3. Radiant heating

Radiant heating is an efficient way to heat a house. The main advantages of radiant heating compared to conventional heating systems are efficiency and comfort for the inhabitants. These characteristics make it attractive and feasible to implement this heating technique coupled with solar collectors.

www.manaraa.com

The computer program in Appendix A includes a function that computes heating loads for inputted ambient temperatures. This program works with the heating load calculations program.

Heated space is divided into three zones with separate radiant heating inputs. This is a common practice in order to avoid high temperatures at the beginning of the loop and low temperatures at the end of the loop. Also, it takes into account room designations. A three-zone system will give us a good approximation of water temperature that is required to input into the radiant heating system's manifold.

Assuming water is used as a working fluid, upward heat flux can be calculated as [17]:

$$q_u = \frac{design\ heat\ load\ of\ space}{availible\ floor\ area\ of\ space} \qquad (4.4)$$

And downward heat flux as: $\frac{Btu\ hr}{ft^2}$:

$$q_d = \frac{4.17(P_e)(T_{slab} - T_{outside})}{(R_{edge} + 5)A} \qquad (4.5)$$

Where:

- $P$ is the exposed perimeter of the slab, ft;
- $T_{slab}$ is the estimated operating temperature of the floor slab at design conditions, F;
- $T_{outside}$ is the ambient temperature, F;
- $R_{edge}$ is the R-value of edge, $\frac{Btu\ hr}{ft^2}$;

www.manaraa.com

- A is the available floor area of the space, $ft^2$.

The outlet water temperature can be estimated as:

$$T_{out} = T_{room\,air} + (T_{in} - T_{room\,air})e^{-b}$$
$$b = \frac{a\,L}{500\,f} \qquad (4.6)$$
$$a = \frac{1}{R_s + R_{ff} + R_{air\,film}} + \left(1 + \frac{q_d}{q_u}\right)$$

Where:

- $T_{in}$ is the room temperature, 68 F;
- $R_s$ is the slab resistance, Btu/(h ft °F);
- $R_{ff}$ is the total thermal resistance of the finished floor materials, Btu/(h ft °F); $R_{air\,film}$ is the air film resistance on the surface of the floor, Btu/(h ft °F); L is the length of the piping circuit, ft; f is the flow rate through the circuit, usgpm.

### 4.3.1. Ventilation

Even though radiant heating is a better way to heat space than more common means of space heating, it does not provide fresh air for the house; therefore, a small ventilation system must be installed. An ASHRAE requirement for the amount of fresh air per person is 15 cubic feet per minute (cfm) [6]. Assuming there are four people in the family, the ventilation flow rate is 55 cfm (30 % fresh air, 70% reused). To provide for the heating of 18 cfm of air to the house, an additional heat exchanger and fan have been added to the system.

www.manaraa.com

## 4.4. Programming

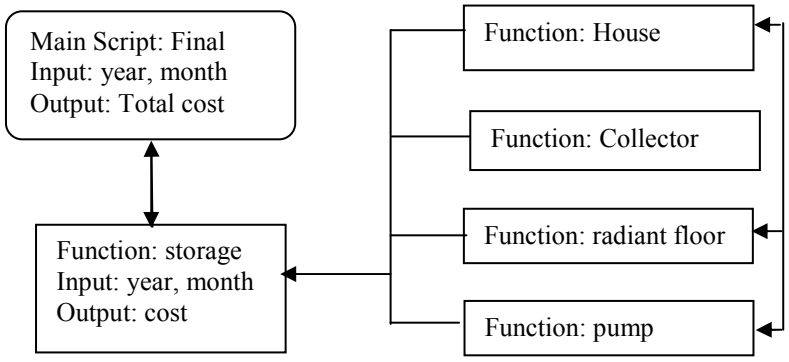


*Figure 22: Flow chart of the simulation*

The flow chart of the main program is presented in Figure 22. Several Matlab functions are not included in the flow chart since their influence on the final results is indirect. The main script of the simulation calculates the useful heat that is produced by the solar heating system and, in case of insufficient radiation levels, activates the electric heating system that plays the role of a backup system in this event.

The available solar radiation data for simulation are the mean monthly [and] daily global radiation for 22 years from 1969 to 1991, and the average number of hours of bright sunshine. The available temperature data are the average temperatures for Astana, Kazakhstan (Appendix E).

## 4.5 Economy

Economic considerations are important in terms of evaluating the solar heating system performance. The value of money changes overtime; therefore, we have to consider the factors that influence the total cost of the system. Present worth is the

www.manaraa.com

difference between the project cost and the heating load worth. The present worth factor can be found as [18]:

$$pwf = \frac{1 - \left(\frac{i+1}{1+dr}\right)^{yr}}{dr - i} \quad (4.7)$$

Where:

- I is the interest rate;
- dr is the discount rate;
- yr is the life of project.

The capital cost was estimated based upon the solar collectors' manufacturer price guides. Operation and maintenance cost are assumed to be negligible.

*Table 5: Economic parameters [1]*

| Parameter | Value |
|---|---|
| electricity cost, $ | 0.05 |
| discount rate | 0.1 |
| life of the project, years | 22 |
| general inflation rate | 0.08 |
| fuel inflation rate | 0.013 |

The present worth for this particular project can be found by:

$$Pw_{solar} = Pw_{Q_{load}} - Pw_{equipment} - Pw_{electr}$$
$$Pw_{electric} = Pw_{Q_{load}} - Pw_{equipment} - Pw_{electr} \quad (4.8)$$

Where:

- $Pw_{solar}$ is the present worth of a solar space heating system;

www.manaraa.com

- $Pw_{electric}$ is the present worth of an electric space heating system;
- $Pw_{Q_{load}}$ is the present worth of heating loads;
- $Pw_{equipment}$ is the present worth of the equipment;
- $Pw_{electr}$ is the present worth of the consumed electricity.

www.manaraa.com

## 5. ANALISYS AND RESULTS

The simulation of the solar heating system (Figure 21, Figure 22) showed that acceptable trends were met. From the beginning it was assumed that a solar heating system would reduce electricity consumption. Figure 23 compares the consumed electricity price trends of a solar space heating system and an electric heating system of the same size for an average year. At this point it is clear that solar heating system consumes less electricity for its needs, which is expected.

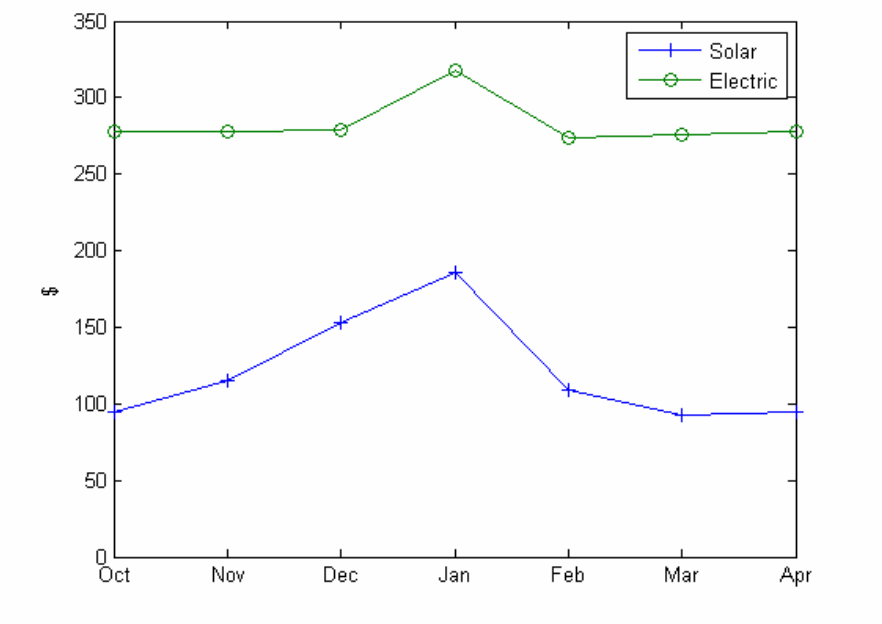


*Figure 23: Cost comparison for an average year*

According to the results of the simulation, the outside air temperature influenced the operating cost in an obvious way in Figure 23. Even though February is the coldest month [6], the January heating load is larger due to the lower average temperature used in heating load calculations. Hence, the operating cost is the highest in January ($325/175).

www.manaraa.com

In summary the resulting savings showed that total savings during the time of the simulation (22 years) due to solar energy implications was $ 22,660. Calculations of the capital cost showed that the current retail price of the G series solar collectors is in the same range as the total savings for 22 years (the capital cost is $ 22,976). These numbers illustrate the present high price of solar collector arrays that halt development of this technology on a larger scale.

The most useful objective function for estimating the performance of asolar heating system is the present worth of the heating system. The present worth of a residential heating system is always negative since it does not produce energy for sale. Table 6 represents the present worth values for solar and electric heating systems.

*Table 6: Present worth of heating systems*

| | |
|---|---|
| Electricity cost, $/kWh | 0.05 |
| Present worth of solar heating system, $ | -17,093 |
| Present worth of electric heating system, $ | -15,778 |

The current price of the G series solar collector is too high for use as an alternative to conventional heating systems. However, performance of this type of collector can be considered as one of the best in the class of flat-type solar collectors (due to Solarstrips technology). In addition, the availability of this type of solar collector in Kazakhstan is questionable. The closest manufacturers of solar collectors to Kazakhstan are located in China. Considering the low labor costs in China, Chinese solar collectors can provide less expensive alternatives and, consequently, improve the feasibility of a flat-type solar collector heating system.

www.manaraa.com

Table 7 shows that results of capital cost optimization and the critical price for the solar heating system with current electricity costs (0.05$/kWh). The critical cost of 700 $/collector means that a solar heating system is more feasible than an electric heating system of the same size if the cost solar collectors is less than 700 $ per collector.

*Table 7: Present worth of heating systems*

| Collector price, $ /collector | Present worth, $ | |
|---|---|---|
| | Electric heating system | Solar heating system |
| 840 | -15778 | -17093 |
| 700 | -15778 | -14693 |
| 600 | -15778 | -12293 |

The other important parameter for estimating the performance of solar heating systems is the need for a back up system. Figure 24 shows the relationship between solar heating systems and electric backup systems. The ratio of the backup system load to the solar heating load can help us to measure the backup system. Overestimating the load of a backup system is a common mistake that leads to the increased capital cost and the overall cost inefficiency of the heating system.

According to Figure 24, the size of the backup system should provide 50 % of a heating load on January (the upper line value). For instance, the heating load in January is 50,000 Btu/h (the heating load does not change since ambient temperatures are assumed to be the same); therefore, the backup system should provide 25,000 Btu/h (7.33 kW).

www.manaraa.com

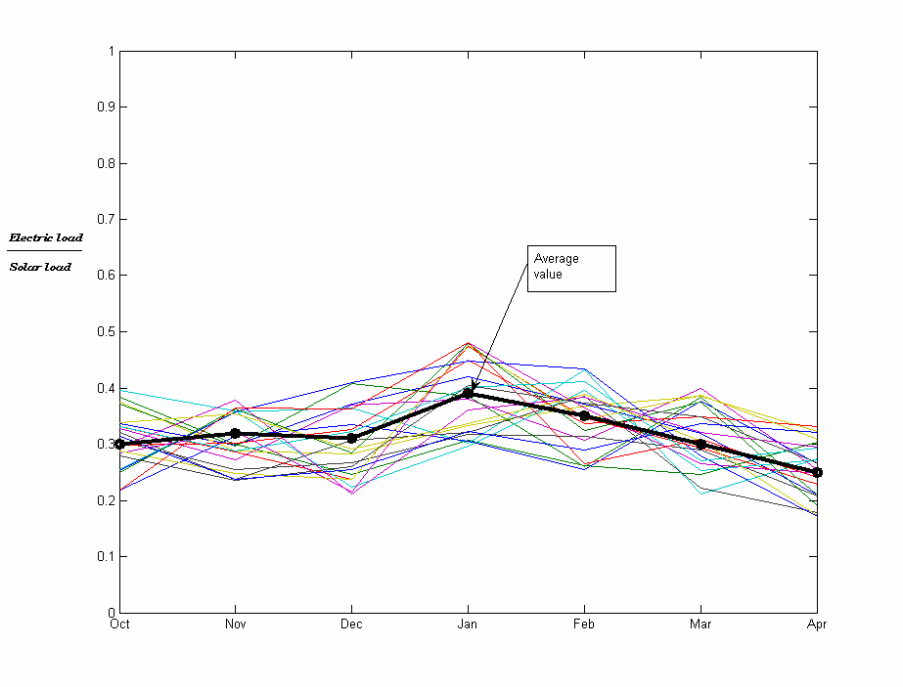


*Figure 24: Ratios of back up system load to solar heating system load (22 years of simulation)*

The backup system can be designed to completely supply the heating load in case of bad weather conditions that cause low solar energy input into the system. However, storing thermal energy makes the system more reliable and independent of weather conditions. A 1000 kg sensible thermal storage tank has been used in simulation. In reality, a storage tank can consist of several tanks connected in a series. Several research studies have been done on simulating sensible thermal storage [7, 9, 15], the results of which verify that three thermal storage collectors connected in a series can provide the same thermal storage capacity as one storage tank of three times size [15].

The fact that the cost of electricity tends to increase the present worth of a solar heating system was analyzed with different electricity costs. Figure 25 was made based on data in Table 8 to show trends in present worth values for different electricity costs.

www.manaraa.com

The present worth of heating systems drastically increases with the increase of electricity rates; however, an electricity cost greater than 0.2 $/kWh is highly unlikely since a quadrupled electricity price will likely initiate the development of alternative technologies that will halt the increase.

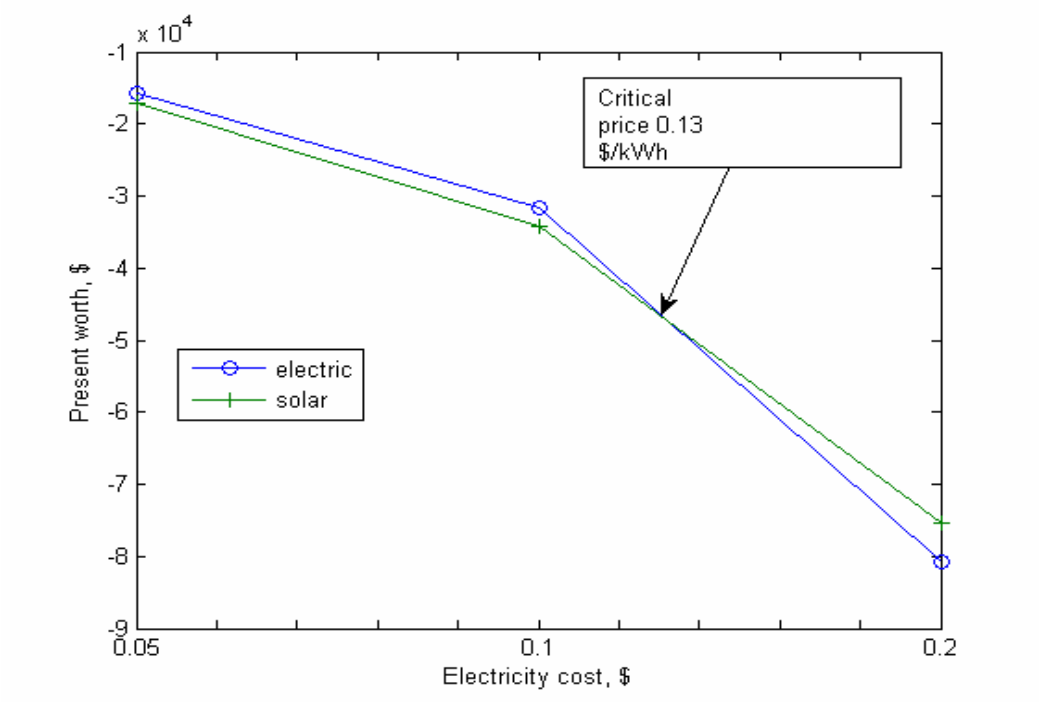


*Figure 26: Present worth of a solar space heating system and an electric heating system with different electricity costs.*

*Table 9: Present worth of solar space heating system and electric heating systems*

| Electricity cost $/kWh / System | 0.05 | 0.1 | 0.2 |
|---|---|---|---|
| Electric heating system | -15,778 | -31,556 | -80,667 |
| Solar heating system | -17,093 | -34,186 | -75,336 |

www.manaraa.com

Figure 25 and Table 8 show that this simulated solar heating system would be feasible if the electricity rate were to increase as high as 0.13 $/kWh. This price is already a reality of the megapolises of the world; however, considering coal resources and population, Kazakhstan will probably not arrive at this point in the near future.

www.manaraa.com

## 6. CONCLUSION

A study of flat-type solar space heating for a residential building has been done. The results show that flat-type solar collectors can perform well under the severe weather conditions and the radiation levels of Astana. However, the simulation of a solar space heating system compared to an electric resistance heating system showed that the solar heating system that is simulated cannot provide enough heating capacity to heat the building without 50 % backup system. In addition, the cost analysis showed that the present worth of the solar heating system can be greater than the electric heating system if the price of solar collectors is less than their current value.

The purpose of this study was to test if the implications of a flat-type liquid-type solar heating system of a typical residential building would be feasible with current electricity. The simulation *disproved* that statement and showed that the current savings and capital cost of a solar heating system is in the same price range which means that not many home owners will risk installing a solar heating system.

In addition, the electricity rate analysis demonstrated that the present worth of the simulated solar heating system is influenced by electricity rates. One of the ways of canceling this relationship is by combining several alternative energy technologies, such as ground-coupled heat pumps, wind power and biogas, with solar space heating systems. This would set aside the present worth of a solar heating system from electricity rates so that the only factor that would need to be improved would be the capital cost.

Solar space heating technology cannot provide an adequate heating load for a residential building in arid, cold climates without a significant increase in efficiency and

www.manaraa.com

size of solar collectors or thermal storage, all of which would lead to increasing the capital cost of the system.

Despite the simulation results, more comprehensive simulations and possibly full scale tests should be performed to verify or disprove these results.

### 6.1. Future work

The residential building that is used in the simulation is a typical residential house without any modifications for improving energy efficiency; therefore, better results could be achieved by improved insulation technologies or passive solar energy technologies.

Computer simulations of solar space heating can provide good approximations and ways of improving efficiency. However, nothing can replace carefully performed experimentation. Experimental work and the collection of detailed data is a priority for future investigation. There is a lot of work on the collection of solar radiation and other types of data that must be done on a larger scale in order to justify solar energy use (creating online solar and wind maps, improving the accessibility of this information, and so on.).

The example of the developed countries, such as the USA, shows that the promotion of alternative technologies, which is an important part of the proliferation of solar energy use, has to be supported by the government. Henceforth, the propagation of alternative energy technologies in Kazakhstan will depend on the lobbying efforts of interested parties and leaders.

www.manaraa.com

## REFERENCES


[1] *Kazakhstan: General information* (n.d.). Retrieved January 07, 2007, from http://missions.itu.int/~kazaks/eng/kazak01.htm

[2] *Kazakhstan: General information (n.d.).* Retrieved January 07, 2007, from http://www.powerexpo.kz/en/2005/desc/

[3] *World Map of the Köppen-Geiger climate classification updated.* Retrieved May 13, 2007, from http://koeppen-geiger.vu-wien.ac.at/

[4] *Summary of SRCC Certified Solar Collector and Water Heating System Ratings (n.d.).* Retrieved May 07, 2007, from http://solar-rating.org/ratings/ratings.htm

[5] *Residential house drawings and supplementary information are provided by Russell Walters, Ph.D., P.E. Iowa State University.*

[6] ASHRAE Handbook (2005). Fundamentals Volume. American Society of Heating, Refrigeration and Air-conditioning Engineers. NY: 2005.

[7] Duffie, J., & Beckman, W. (2006). Solar engineering of thermal processes, 3rd Ed., New York: John Wiley & Sons

[8] *Radiation data for Kazakhstan.* Retrieved January 10, from http://www.worldclimate.com/cgi-bin/data.pl?ref=N51E071+2100+35188W

[9] Tiwari G.N. (2002). Solar Energy: Fundamentals, Design, Modeling and Applications. New Delhi: Narosa Publishing House

[10] *G series solar collectors: specifications.* Retrieved April 1, 2007, from http://www.thermo-dynamics.com/technical_specs/G_series_technical.html

[11] Incropera, P., &DeWitt, D. (1996). Introduction to Heat transfer, 3rd Ed., New York: John Wiley & Sons


www.manaraa.com

[12] *Water properties: Matlab function.* Retrieved May 13, 2007, from http://www.x-eng.com

[13] *Air properties: Matlab function.* Retrieved May 13, 2007, from http://www.mathworks.com/matlabcentral/fileexchange/loadFile.do?objectId=5165&objectType=file

[14] *Propylene glycol: Properties.* Retrieved May 13, 2007, from http://www.sigmaaldrich.com/catalog/search/ProductDetail/SIAL/P4347

[15] *Experimental analysis of stratified multi-tank thermal storage configurations for solar heating systems*. Retrieved May 13, 2007, from http://www.solar2006.org/presentations/tech_sessions/t23-a046.pdf

[16] Dincer, I., & Rosen, M. (2002).Thermal energy storage., NY: John Wiley & Sons

[17] Siegenthaler, J.,(1995). Modern hydronic heating for residential and light commercial buildings. New York: Delmar Publishers

[18] Burmeister, L., (1998).Elements of thermal-fluid system design., NJ:Prentice-Hall

www.manaraa.com

# Appendix A. Computer program

## A.1. Final script

```
%Economical parameters
Cload=.05;% worth of load
elec=0.3; % electricity cost $/kwh,
dr=0.1; % discount rate
yr=22; % life project
ig=0.08; % general inflation rate
ifu=0.013; % fuel inflation rate
%no loans no salvage values.
pwf=(1/(dr-ig))*(1-((ig+1)/(1+dr))^yr);   % present worth factor
%Capital cost
Nc=24; % number of collectors
Ccol=800; % $ collector cost
HxC=1000; % Heat exchangers estimated cost, $.
Hxa=500; % estimate air glycol cost
Fanc=200; % fan cost
Csto=300; % Storage estimated cost, $
Cc=Nc*Ccol; %Collectors cost, $
Cpg=5*40;% proplelene glycol price $40/gallon
Cpumps=2*504;% 2 pump cost, $
% electric heat cost. 50,000 BTU/h=14.65 KW
Ceh=(550+40*14.65)/2;%electric heater cost.(50%capacity)
CCs=HxC+Csto+Cc+Cpg+Cpumps+Ceh+Hxa+Fanc;%capital cost of solar heating
system
CCe=(Ceh*2)+Cpumps+Hxa+Fanc;          %capital cost of electric heating
system
[Diffuse,Global,Hcb,Ho,Ht_bar,Kt,Hkt,Global_dayly,Diffuse_dayly,Average
persunsh,Na,Rad]=Solar;
cnt1=0;
for y=69:92
    cnt1=cnt1+1;
      %heating season months
for  j=1:4;
    %Calculating
n=24-(ceil(Averagepersunsh(j+1)));
con=0;
[Cost_elec_1,Cost_auxilary_1,pfan,air_cost,q_load]=storage(y,j,n,con,el
ec) ;
%function storage input year and month
%n- number of hours
%con-control function,= 1  for radiation
% or zero for night hours
n=(ceil(Averagepersunsh(j+1)));
con=1;%con-control function,= 1  for radiation
% or zero for night hours
[Cost_elec,Cost_auxilary,pfan,air_cost,q_transf]=storage(y,j,n,con,elec
) ;
Cost_auxilary_total(cnt1,j)=30*((sum(Cost_auxilary)+sum(Cost_auxilary_1
)...
    +(pfan+mean(air_cost))*24*elec));%$/day
Cost_solar(cnt1,j)=30*(sum(Cost_elec_1)+sum(Cost_elec)+(pfan+...
```

www.manaraa.com

```
    (sum(air_cost))))*elec;%$/day
Costload(cnt1,j)=q_load*24*30*Cload*pwf; %worth of heating load
end
cnt=9;
for  j=5:7;
    cnt=cnt+1;
[Diffuse,Global,Hcb,Ho,Ht_bar,Kt,...
Hkt,Global_dayly,Diffuse_dayly,Averagepersunsh,Na,Rad]=Solar;
n=24-(ceil(Averagepersunsh(cnt+1)));
con=0;
[Cost_elec_1,Cost_auxilary_1,pfan,air_cost,q_load]=storage(y,cnt,n,con,
elec) ;
%function storage input year and month
%n- number of hours
%con-control function,= 1  for radiation
% or zero for night hours
n=(ceil(Averagepersunsh(cnt+1)));
con=1;
[Cost_elec,Cost_auxilary,pfan,air_cost,q_transf]=storage(y,cnt,n,con,el
ec);
Cost_auxilary_total(cnt1,j)=30*((sum(Cost_auxilary)+sum(Cost_auxilary_1
)+(pfan+mean(air_cost))*24*elec));%$/day
Cost_solar(cnt1,j)=30*(sum(Cost_elec_1)+sum(Cost_elec)+(pfan+(sum(air_c
ost))))*elec;%$/day
Costload(cnt1,j)=q_load*24*30*Cload*pwf; %worth of heating load
end
end

PW_Sol=((mean(Costload))*7)-((mean(Cost_solar))*pwf*7)-CCs;
PW_elec=((mean(Costload))*7)-((mean(Cost_auxilary_total))*pwf*7)-CCe;
```

**Solar radiation computation program**

```
function  [Diffuse,Global,Hcb,Ho,Ht_bar,Kt...

,Hkt,Global_dayly,Diffuse_dayly,Averagepersunsh,Na,Rad]=Sol
ar
%%Initial data.
% Site Location
Lat=53.15; % LAtitude
Alt=350; % Altitude, meters
Gsc=1367; % Solar Constant W/m^2
%%%%%%%%%%%%%Annual Extraterrestial Radiation on a
horizontal surface%%%%%%%
beta=0; % horizontal plane
gamma=0; % surface azimuth angle (orientation to south
north axe)
```

www.manaraa.com

```
 %%%%%%%Reading Data file for Number of hours of sunshine
1962- 1992  %%%%%
     fid_data=fopen('DAta Sunshine 69-92.txt','r'); %%%
open file for reading
     A=fscanf(fid_data,'%e%e%e%e ', [4 inf]);
     B11=A';
%  Defining arrays
omegas=(1:365);  % sunset hour angle
N=(1:365); % number of days a yeaer
sunset=(1:365);
sunrise=(1:365);
Ho=(1:365);
% Ho -  daily extraterrestial radiation on a horizontal
surface
for h=1:365
omegas(h)=rd(acos(-tan(dr(Lat))*tan(sigma(h)))); % sunset
hour angle degree
N(h)=(2/15)*omegas(h) ;   % number of daylight hours
sunset(h)=(omegas(h))/15; % sinset hour angle
sunrise(h)=sunset(h)*(-1);% sunrise hour angle
Ho(h)=(24*3600*Gsc/pi)*(1+0.033*((cos(dr(360*h/365)))))*...
 ((
(cos(dr(Lat)))*((cos(sigma(h)))*((sin(dr(omegas(h)))))+..
.
 (dr(omegas(h)))*((sin(dr(Lat))))*((sin(sigma(h)))));
% Ho -  daily extraterrestial radiation on a horizontal
surface
end
f=Ho; %%Intermidate variable
Ho=f*10^(-6);  %%Converting to MJ/m^2
i=0;j=0;
for h=1:22  % 22 is a number of years of data
    j=j+1;
     mon(h,1)=B11(j,1);
        for k=2:13
            i=i+1;
            mon(h,k)=B11(i,4);

        end
   j=j+12;
end

% Monthly average daily hours of bright sunshine
[m,n] = size(mon);
for h=2:13
mon(23,h)=(mean(mon(1:m,h)));
```

www.manaraa.com

```
end

% Monthly average of maximum possible daily hours of bright
sunshine
Avedays=[17,47,75,105,135,162,198,229,259,288,318,344];%AVe
rage days of months
for h=1:12
Na(h)=(2/15)*(rd(acos(-
tan(dr(Lat))*tan(sigma(Avedays(h))))) ;
noverN(1,h)=mon(23,h+1)/Na(h);
noverN(2,h)=noverN(1,h)*100; % percents
end
for i=2:13%from 2 since first row is a year
Averagepersunsh(i)=mean(mon(1:23,i)); %% average number of
hours of  sunshine.

end
%%%%%%Estimation of clear sky radiation%%%%%%%%%%
a0=0.4237-0.00821*(6-(Alt*10^(-3)))^2;
a1=0.5055+0.00595*(6.5-(Alt*10^(-3)))^2;
ks=0.2711+0.01858*(2.5-(Alt*10^(-3)))^2;
        %correction factors for Climate Types (subarctic
summer.)
R0=0.99;
R1=0.99;
Rk=1.01;

for n=1:365
    %%%Extraterrestial radiation incident on the plane
normal to the
       %%%radiation on the nth day of year
       B=(n-1)*360/365;

Gon(n)=Gsc*(1.000110+0.31221*cos(dr(B))+0.001280*sin(dr(B))
+...
       0.000719*cos(2*dr(B))+0.000077*sin(2*dr(B)));
       sunsetrise=round(sunset(n)); % rounding number of
hours before/after solar noon
       om=-7.5 ;%half an hour after the sunrise

       for i=1:sunsetrise
           omega=om;

cosz=(cos(dr(Lat))*cos(sigma(n))*cos(dr(omega))+sin(dr(Lat)
)...
               *sin(sigma(n)));
```

www.manaraa.com

```
            %%% Atmospheric transmittence for beam radiation
            tb=a0*R0+a1*R1*exp(-ks*Rk/cosz);
            om=omega-15; %% step one hour
            taub(i)=tb;
            %%%%%%% The beam radiation on a horizontal plate
            Gcnb(n,i)=Gon(n)*taub(i);
            Gcb(n,i)=Gon(n)*taub(i)*cosz;
            taud(n,i)=0.271-0.294*taub(i);
            Gcd(n,i)=Gon(n)*cosz*taud(n,i);
            Icnb(n,i)=Gcnb(n,i)*3600;  %%Mj/m2
            Icb(n,i)=Gcb(n,i)*3600;
            Icd(n,i)=Gcd(n,i)*3600;
         end
         %%%%  Daily beam radiation clear sky.
         %%%%  Mj/m2!!!!!!!!!!!!!!!!!!!!!!!!!!!!!!!!!!
       Hcb(n)=(2*(sum(Icb(n,1:sunsetrise))))*10^(-6);

end
%Reading Global Radiation from file
 fid_data=fopen('Global.txt','r'); %%% open file
     C1=fscanf(fid_data,'%d',[4 inf]);
     C=C1.';
     clear ('C1');
     [g,n]=size(C);

  %      Average for years
      for i=1:12
          d=0;cnt=0;
          for k=1:g
            if C(k,2)==i
               d=d+C(k,4);
               cnt=cnt+1;
            end
          end
          d1=d/cnt;
          Global(i)=0.01*d1; % monthly sums MJ/m2
      end

 clear ('C');
%Organize data. Mean values
%Extraterretrial rad sums
f3(1)=sum(Ho(1:31));f3(2)=sum(Ho(32:59));f3(3)=sum(Ho(60:90
));
f3(4)=sum(Ho(91:120));f3(5)=sum(Ho(121:151));f3(6)=sum(Ho(1
52:181));
```

www.manaraa.com

```
f3(7)=sum(Ho(182:212));f3(8)=sum(Ho(213:243));f3(9)=sum(Ho(
244:273));
f3(10)=sum(Ho(274:304));f3(11)=sum(Ho(305:334));f3(12)=sum(
Ho(335:365));
 %%%Clear sky
 clear ('f');
f(1)=sum(Hcb(1:31));f(2)=sum(Hcb(32:59));f(3)=sum(Hcb(60:90
));
f(4)=sum(Hcb(91:120));f(5)=sum(Hcb(121:151));f(6)=sum(Hcb(1
52:181));
f(7)=sum(Hcb(182:212));f(8)=sum(Hcb(213:243));f(9)=sum(Hcb(
244:273));
f(10)=sum(Hcb(274:304));f(11)=sum(Hcb(305:334));f(12)=sum(H
cb(335:365));
 %%%%Comparison.  F3 and T

 % Reading diffuse radiation from file
fid_data=fopen('diffuse 90- 92.txt','r'); %%% open file
     C1=fscanf(fid_data,'%d',[3 inf]);
     C=C1.';
     clear ('C1');
     [g,n]=size(C);

  %      one year
      for i=1:12
          d=0;cnt=0;
          for k=1:g
            if C(k,2)==i
               d=d+C(k,3);
               cnt=cnt+1;
            end
          end
          d=d/cnt;
          Diffuse(i)=0.01*d; % monthly sums MJ/m2
      end

  clear ('C');


% Monthly average isotropic-sky radiation on a sloped
surface.

rho_g=[.7,.7,.7,.4,.2,.2,.2,.2,.2,.2,.4,.7,.7]; %Ground
reflectance (Assumed)
```

www.manaraa.com

```
% %%%Clearness index
Kt=Global./f3;

for m=1:12
          if     m==1
              n=17;
          elseif m==2
              n=47;
          elseif m==3
              n=75;
          elseif m==4
              n=105;
          elseif m==5
              n=135;
          elseif m==6
              n=162;
          elseif m==7
              n=198;
          elseif m==8
              n=228;
          elseif m==9
              n=258;
          elseif m==10
              n=288;
          elseif m==11
              n=318;
          elseif m==12
              n=344;


          end
          om1=acos(-tan(dr(Lat-beta ))*tan((sigma(n))));
      om2=acos(-tan(dr(Lat))*tan((sigma(n))));
      SUnset_angle_on_collec=min(om1,om2);

      R_b(m)=((cos(dr(Lat-beta))*cos(sigma(n))*...
          sin(SUnset_angle_on_collec)) +...
          (pi*((rd(SUnset_angle_on_collec))/180)*sin(dr(Lat-
beta))*sin(sigma(n))))/...
          ((cos(dr(Lat))*cos(sigma(n))*...
          sin(SUnset_angle_on_collec)) +...

(pi*((rd(SUnset_angle_on_collec))/180)*sin(dr(Lat))*sin(sig
ma(n))));
```

www.manaraa.com

```
        Ht_bar(m)=(Global(m)-
Diffuse(m))*R_b(m)+Diffuse(m)*rho_g(m)*(1+cos(dr(beta))/2)+
...
         Global(m)*(1-cos(dr(beta))/2);                    %
MJ/m2

end

beta=70;
%%%%KT model
Hkt=KT(Lat,beta,Ho,Diffuse,Global,Kt,gamma);
%Absorbed radiation
%param=[Lat,Global,Diffuse];
%Reading monthly daily mean
 fid_data=fopen('Global.txt','r'); %%% open file
     C1=fscanf(fid_data,'%d',[4 inf]);
     C=C1.'; %transposition
     clear ('C1','d','cnt');
     [g,n]=size(C);
      for i=1:12
           d=0;cnt=1;
          for k=1:g-12
            if C(k,2)==i
               C1(cnt)=C(k,3);
               cnt=cnt+1;
            end
          end
          Global_dayly(i)=0.01*(mean(C1)); % monthly dayly
means MJ/m2
      end
%Collare-Pereira and Rabl correlation for diffuse radiation
estimation
%page  77,[3]

  for i=1:12
      if Kt(i)<=0.17
          Diffuse_dayly(i)=Global_dayly(i)*0.99;
      elseif ((Kt(i) > 0.17) && (Kt(i) < 0.75))
        Diffuse_dayly(i)=Global_dayly(i)*(1.188-
2.272*Kt(i)+9.473*Kt(i)*...
           Kt(i)-21.865*(Kt(i))^3+14.648*(Kt(i))^4) ;
      elseif ((Kt(i) > 0.75) && (Kt(i) < 0.80))
         Diffuse_dayly(i)=Global_dayly(i)*(-
0.54*(Kt(i))+0.632);
      elseif Kt(i) >= 0.80
           Diffuse_dayly(i)=Global_dayly(i)*0.2;
```

www.manaraa.com

```
      end
  end

%%%DEfining arrays of GLobal radiation 1964-1991
% converting data from MJ/m2 to W/m2
% B11- sunshine hours
% C- global radiation
[m1,n1] = size(C);
[m2,n2] = size(B11);
cnt=0;
for i=61:m2
    cnt=cnt+1;%counter
    if C(i,1)==B11(cnt,1) && C(i,2)==B11(cnt,2)%matching
availible data for
        %radiation nad number of hours of sunshine and
converting global
        %radiation to instantenious values, W
        %%Separating diffuse froom global radiation using
Collare-Pereira correlation
        if Kt(C(i,2))<=0.17 % average values of Kt
          Diffuse_d(i)=C(i,3)*0.99;
      elseif ((Kt(C(i,2)) > 0.17) && (Kt(C(i,2)) < 0.75))
        Diffuse_d(i)=C(i,3)*(1.188-
2.272*Kt(C(i,2))+9.473*Kt(C(i,2))*...
            Kt(C(i,2))-
21.865*(Kt(C(i,2)))^3+14.648*(Kt(C(i,2)))^4) ;
      elseif ((Kt(C(i,2)) > 0.75) && (Kt(C(i,2)) < 0.80))
         Diffuse_d(i)=C(i,3)*(-0.54*(Kt(C(i,2)))+0.632);
      elseif Kt(C(i,2)) >= 0.80
          Diffuse_d(i)=C(i,3)*0.2;
        end
      %%Combined values for global radiation and diffuse
radiation average
      % daily sums, MJ/m2.
    Rad (cnt,2) =Diffuse_d(i);

    Rad (cnt,1) =C(i,3);
    Rad (cnt,3) =B11(cnt,1);
    end


end
```

www.manaraa.com

## A.2. Radiant floor program

```
function [Tout,f,Q]=radiant_floor(i,Tin)% month,
temperature, F
Sei=11; %Slab edge insulation R-11
t=4; %slab thickness ,inches
Rff=0.21; %%floor finish vinil tile
R_air_film=0.61; % assumed
Rs=0.795; %Slab resistance, graph.
A1=1534;  %Area
A=A1*0.7; %aproximate open floor. 70% of the floor is not
covered
%Outside temperature
F =[-6.8,-6.6,4.6,28,42.4,52.3,56.3,51.8,41.4,28.6,12,-1];
%°F
% Radiant floor
L=61; %feet
W=25;  %feet
f=1.5; % flow rate gpm
%3/4 in plastic tubing spaced 12 ins on center
Np=23; % number of pipes ASsumed from the geometry of the
building
qload=house(i); % heating load, BTU/h
q_u=(qload)/A; % Upward heat flux.
p=1; % initial guess
while (q_u-p)>1
Tw=68+q_u*(Rs+Rff+R_air_film); %Average water temperature
required in a circle, F.
q_d=(4.17*(L+W)*(Tw-F(i)))/((Sei+5)*(1534));
a=(1/((Rs+Rff+R_air_film)))*(1+(q_d/q_u));
b=a*60*Np/(500*f);
Tout=68+(Tin-68)*exp(-b);
Q=500*f*(Tin-Tout); % total heat flux, Btu/h
p=(Q-q_d);
f=f-0.1;% new flow rate
end
```

www.manaraa.com

## A.3. Calculation of overall heat loss coefficient, useful gain, and outlet water temperature.

```
function [U_l,Tmp,Q_u,Tfo]=U_l(i,Tin,beta,Sbar_w_per_m2)
Tmp=Tin+50; % mean plate , initial guess, C
Cel =[-21.6,-21.5,-15.2,-2.2,5.8,11.3,13.5,11,5.2,-1.9,-
11.1,-18.4];  % °C
sigma=5.6*10^(-8); %Stefan-boltzman constant
V=10; % Wind speed Assumed m/s
e_p=0.95;  %plate emmitance
e_g=0.88; %glass emmitance
t_b=0.025; %m
k_b=0.036;%W/mC
p_c_t=0.025; %m
rho_gl=1036;% kg/m3
m_dot=2.5; %Assumed flow rate in the collector, L/m
mdot_gl=m_dot*rho_gl/3600; % flow rate  , kg/s
A_coll=4*2.96; % Area of a collector  ,m
Coll_length=2.47;  %m
h_fi=300;% initial guess  heat transfer coefficient
D_h=4*120/36;% hydraulic diameter
Ta=Cel(i); % ambient temperature
Tsky=Ta-6;% sky temperature
Tg=Ta+20; %Assumed glass temperature,C
Tg1=Tg+15; %Tg1 always bigger to get results.
e_eff=((1/e_p)+(1/e_g)-1)^(-1 ); %effective emmisivity of
plate glasing system;
while (Tg-Tg1)<2   % Loop break condition
Tg=Tg1;
h_r_1=e_eff*sigma*( (Tmp+273)^4-(Tg+273)^4 )/(Tmp-Tg);
% radiation transfer coefficient, plate to cover
h_r_2=e_g*sigma*( (Tg+273)^4-(Tsky+273)^4 )/(Tg-Ta);
%radiation transfer coefficient, cover to sky
% Air properties @ film temperature
T_film=(((Tmp+273)+(Tg+273))/2);
kond_a=airProp2(T_film ,'k' );
ny=airProp2(T_film, 'ny');
alfa_a=kond_a/(airProp2(T_film, 'rho')*airProp2(T_film,
'cp'));
    Ra=9.81*(Tmp-
Tg)*(1/T_film)*(0.025)^3/(alfa_a*ny);%rayleigh number
    if beta<=75
    B1=1-(1708/(Ra*cos(dr(beta))));
    B2=((Ra*cos(dr(beta))/5830)^(1/3))-1;
```

www.manaraa.com

```
        if B1<0
          B1=0;
        end
        if B2<0
            B2=0;
        end
    Nu=1+1.44*B1*(1-
(sin(dr(1.8*beta)^(1.6)))*1708/(Ra*cos(dr(beta))))+B2;
    elseif beta>75
        A=Coll_length/p_c_t;%ratio of plate length to space
to absorber
        B1=0.288*(Ra*sin(dr(beta))/A)^(1/4);
        B2=0.039*(Ra*sin(dr(beta)))^(1/3);
        Nu=max(B1,B2);
        if B1<1 && B2<1
            Nu=1;
        end
    end
h_c_1=Nu*kond_a/p_c_t;
h_c_2=2.8+3*V;
U_t=((1/(h_r_1+h_c_1))+(1/(h_r_2+h_c_2)) )^(-1);
Tg1=Tmp-(U_t/(h_c_1+h_r_1))*(Tmp-Ta);
U_b=k_b/t_b;                %back loss coefficient,W/m2C
A_e=(1.20+2.47)*2*0.086;    %edge area
U_e=U_b*(A_e/A_coll);       %edge loss coefficient,W/m2C
U_l=U_t+U_b+U_e;            %Overall top loss coefficient,
W/m2C
Cp_gl=3806;                  %specific heat poly glycol
J/kgK
S=Sbar_w_per_m2;            %absorbed radiation, W/m2
m=(U_l/(0.0005*385))^(1/2); % plate thermal conductivity
and thickness
F=(tanh(m*(0.143-0.012)/2 ))/(m*(0.143-0.012)/2 );
F_r_s=(1/U_l)/(0.143*(1/(U_l*(0.012+(0.143-
0.012)*F))+1/(pi*0.04*h_fi)));
F_r=(mdot_gl*Cp_gl/(A_coll*U_l))*(1-exp(-
(A_coll*U_l*F_r_s/(mdot_gl*Cp_gl))));
Q_u=A_coll*F_r*(S-U_l*(Tin-Ta));                    %%actual
useful gain
Tmp=(Tin+((Q_u/A_coll)/(F_r*U_l))*(1-F_r));% mean plate
temperature , C
Tfo=((Q_u/U_l)+Ta)+(Tin-Ta-(Q_u/U_l))*exp(-
A_coll*U_l*F_r_s/(mdot_gl*Cp_gl));%output water temperature
mu_gl=3.1*10^(-3); %m2/s
nu_gl=mu_gl/rho_gl;
k_gl=0.34 ;                 %W/m-K  50% H2O @90°C
```

www.manaraa.com

```
alfa=k_gl/(rho_gl*Cp_gl); % thermal diffusivity
Pr=nu_gl/alfa; % Prandtl Number
Re=4*mdot_gl/(pi*D_h*10^(-3)*mu_gl); %Reynolds NUmber
f=(0.79*log(Re)-1.64)^(-2);% Darcy friction factor
Nu_gl=(f/8)*(Re-1000)*Pr/(1+12.7*((f/8)^.5)*((Pr^(2/3))-
1));
h_fi=Nu_gl*k_gl/(D_h*10^(-3));% heat transfer coefficient
inside tubes, w/mC
end
```

### A.4. Absorbed radiation program.

```
function
[Sbar,Sbar_w_per_m2]=absorbed(beta,param,Averagepersunsh,Na
)
 Lat=param(1);
 Global(1:12)=param(2:13);
 Diffuse(1:12)=param(14:25);
 rho_g=[.7,.7,.7,.4,.2,.2,.2,.2,.2,.2,.4,.7,.7]; %Ground
reflectance (Assumed)
 N=1;%number of covers
l_g=0.0038; %glass thickness, m
KL=4*l_g;
   for m=1:12
         if     m==1
             n=17;
         elseif m==2
             n=47;
         elseif m==3
             n=75;
         elseif m==4
             n=105;
         elseif m==5
             n=135;
         elseif m==6
             n=162;
         elseif m==7
             n=198;
         elseif m==8
             n=228;
         elseif m==9
             n=258;
```

www.manaraa.com

```
        elseif m==10
            n=288;
        elseif m==11
            n=318;
        elseif m==12
            n=344;
        end

[tau_alfa_g,tau_alfa_d,tau_alfa_b]=transmittence(beta(m),N,
KL);
    om1=acos(-tan(dr(Lat-beta(m) ))*tan((sigma(n))));
    om2=acos(-tan(dr(Lat))*tan((sigma(n))));
    SUnset_angle_on_collec=min(om1,om2);
R_b(m)=((cos(dr(Lat-
beta(m)))*cos(sigma(n))*sin(SUnset_angle_on_collec))+...
        SUnset_angle_on_collec*sin(dr(Lat-
beta(m)))*sin(sigma(n)))/...

(cos(dr(Lat))*cos(sigma(n))*sin(SUnset_angle_on_collec)
+...

SUnset_angle_on_collec*sin(dr(Lat))*sin(sigma(n)));
Sbar(m)=(Global(m)-
Diffuse(m))*R_b(m)*tau_alfa_b(m)+Diffuse(m)*tau_alfa_d*...
((1+cos(dr(beta(m))))/2)+Global(m)*tau_alfa_g*rho_g(m)*((1-
cos(dr(beta(m))))/2);
Sbar_w_per_m2(m)=((Global(m))*(10^6/(Averagepersunsh(m+1)*3
600))-...
Diffuse(m)*(10^6/(Na(m)*3600)))*R_b(m)*tau_alfa_b(m)+Diffus
e(m)*(10^6/(Na(m)*3600))*tau_alfa_d*...
((1+cos(dr(beta(m))))/2)+Global(m)*(10^6/(Na(m)*3600))*tau_
alfa_g*rho_g(m)*((1-cos(dr(beta(m))))/2);
% absorbed radiation for
 end
```

## A.5. Calculation of an optimum slope for incident radiation Isotropic-sky model.

```
function  Hmax=sloped_iso(beta,param,month)
m=month;
%param=[Kt,Lat,Global,Diffuse];
Lat=param(1);
```

www.manaraa.com

```
Global(1:12)=param(2:13);
Diffuse(1:12)=param(14:25);
rho_g=[.7,.7,.7,.4,.2,.2,.2,.2,.2,.2,.4,.7,.7]; %Ground
reflectance (Assumed)

          if     m==1
              n=17;
          elseif m==2
              n=47;
          elseif m==3
              n=75;
          elseif m==4
              n=105;
          elseif m==5
              n=135;
          elseif m==6
              n=162;
          elseif m==7
              n=198;
          elseif m==8
              n=228;
          elseif m==9
              n=258;
          elseif m==10
              n=288;
          elseif m==11
              n=318;
          elseif m==12
              n=344;


          end
      om1=acos(-tan(dr(Lat-beta ))*tan((sigma(n))));
      om2=acos(-tan(dr(Lat))*tan((sigma(n))));
      SUnset_angle_on_collec=min(om1,om2);
R_b(m)=((cos(dr(Lat-
beta))*cos(sigma(n))*sin(SUnset_angle_on_collec))+...
          (SUnset_angle_on_collec*sin(dr(Lat-
beta))*sin(sigma(n))))/...

((cos(dr(Lat))*cos(sigma(n))*sin(SUnset_angle_on_collec))
+...

(SUnset_angle_on_collec*sin(dr(Lat))*sin(sigma(n))));
Ht_bar=(Global(m)-
Diffuse(m))*R_b(m)+Diffuse(m)*((1+cos(dr(beta)))/2)+...
```

www.manaraa.com

```
        Global(m)*rho_g(m)*((1-cos(dr(beta)))/2);


Hmax=1/Ht_bar;
```

## A.6. Calculation of transmittance of glass.

```
function
[tau_alfa_g,tau_alfa_d,tau_alfa_b]=transmittence(beta,N,KL)
theta_g=dr(90-0.5788*beta+0.002693*beta^2);
theta_d=dr(59.7-0.1388*beta+0.001497*beta^2);
theta2=asin(sin(dr(beta))  /1.526); %rad
r_perpen_g=(sin (( theta2-  theta_g)))^2/(sin (( theta2+
theta_g)))^2;
%refractive index  to surface.
r_perpen_d=(sin (( theta2-  theta_d)))^2/(sin (( theta2+
theta_d)))^2;
%refractive index  to surface.
r_paral_g=(tan (( theta2-  theta_g)))^2/(tan (( theta2+
theta_g)))^2;
%refractive index  to surface.
tau_a=exp( -KL /(cos((theta2)))) ;
r_paral_d=(tan (( theta2-  theta_d)))^2/(tan (( theta2+
theta_d)))^2;
tau_d=tau_a/2*( (1- r_paral_d)/(1+(2*N-1)* r_paral_d )+
((1- r_perpen_d)/(1+(2*N-1)* r_perpen_d ))) ;
tau_g=tau_a/2*( (1- r_paral_g)/(1+(2*N-1)* r_paral_g )+
((1- r_perpen_g)/(1+(2*N-1)* r_perpen_g ))) ;
rho_d=tau_a-tau_d;
rho_g=tau_a-tau_g;
alfa_p=1-tau_a;
tau_alfa_g=tau_g*alfa_p/(1-(1-alfa_p)*rho_g);
tau_alfa_d=tau_d*alfa_p/(1-(1-alfa_p)*rho_d);
Lat=53.15;
% mean day of the month
for m=1:12
        if     m==1
            n=17;
        elseif m==2
            n=47;
        elseif m==3
            n=75;
        elseif m==4
            n=105;
```

www.manaraa.com

```
        elseif m==5
            n=135;
        elseif m==6
            n=162;
        elseif m==7
            n=198;
        elseif m==8
            n=228;
        elseif m==9
            n=258;
        elseif m==10
            n=288;
        elseif m==11
            n=318;
        elseif m==12
            n=344;
        end

omega=dr(-2.5*15) ; %radians  % [2],page 229
theta_b=acos(cos(dr(Lat-beta)  )
*cos(sigma(n))*cos(omega)+...
sin (dr(Lat-beta) )*  sin(sigma(n)) );
theta2=asin((sin(theta_b))  /1.526); %rad
%%%beam radiation tau_alfa
r_perpen_b=(sin (( theta2-  theta_b)))^2/(sin (( theta2+
theta_b)))^2;
%refractive index  to surface.
r_paral_b=(tan (( theta2-  theta_b)))^2/(tan (( theta2+
theta_b)))^2;
%refractive index  to surface.
tau_a=exp( -KL /(cos((theta2)))) ;
tau_b=1/2*((1-r_paral_b)/(1+(2*N-1)* r_paral_b )+ ((1-
r_perpen_b)/(1+(2*N-1)* r_perpen_b ))) ;
alfa_p=.90; %absorber plate absorptance independant of
angle
rho_d=tau_a-tau_b;
tau_alfa_b(m) = tau_b*alfa_p/(1-(1-alfa_p)*rho_d)  ;
end
```

## A.7. Heating load calculations

```
function Qload=house(month)
%%%Input desired month
```

www.manaraa.com

```
i=month;
Ceiling=1534; %FT2
doors=2*73; %ft2
Windows=211;%ft2
Garage_Walls=446.4;%ft2
Floor=1534;%ft2
FloorP=214.5;%ft2
exposed_area=2797.2;%ft2
Volume=12272;%ft3
Basement=1534;%ft2
%Design conditions ASHRAE  (2005)
Cl=4840;%Air latent factor,  Btu/h*cfm
Cs=1.1;%Air sensible heat factor,   Btu/h*cfm*F
Ct=4.5;% air total heat factor,  Btu/hrcfm(Btu/lb)
Hro=1.6; % average winter outside Humidity ratio grains of
moisture per lb of dry air.
% WInter
WIndoorT=68;
WIndoorRH=30;%
WOutdoorT=-17.8;
WdeltaT=85.8;
WBasementT=8.9;
WgarageT=-17.8;
%Summer
SIndoorT=75;
SIndoorRH=  30;%
SOutdoorT=85.7;
SDaily_range=19.1;
SOutdoor_wb=62.9;
SdeltaT=10.7;
SMoistureD=0.001;
%%%These values are calculated by ASHRAE  method
%%%Heating loads
Al=116.2; %Ventilation and infiltratioin flow
Qvi=45.34;  %%Combined infiltration/ventilation flow rate.
cfm
deltaW=0.0052;%indoor/outdoor HUmidity ratio difference
gr/lb
hrv_erv=0.7;%heat recovery ventilators and energy recovery
ventilators (HRV/ERVs) effectivness.
%Average minimum Temperatures
    %Jan    Feb Mar Apr May Jun Jul Aug Sep Oct Nov Dec
%C =[-21.6,-21.5,-15.2,-2.2,5.8,11.3,13.5,11,5.2,-1.9,-
11.1,-18.4];  % °C
 F =[-6.8,-6.6,4.6,28,42.4,52.3,56.3,51.8,41.4,28.6,12,-1];
%°F
```

www.manaraa.com

```
 Fmax =[ 10.4 ,11.7, 23.5 ,48.6 ,67.1 ,77.4 ,80.6 ,76.1,
65.5 ,47.5, 26.8 ,14.4 ,45.9 ];
Tif=68;%Internal Temperature °F
Tic=20;%Internal Temperature °C
deltaT=68-F(i);
IDF=(698+8*deltaT*(0.81+0.53*(0.016/116.2)))/1000;%%Infiltr
ation driving force (ASHRAE  2005,p29.5)
Qi=Al*IDF; %Infiltration airflow rate, cfm
ACH=60*Qi/(2905*8)  ;%Air exchange per hour
qvi=Cs*Qvi*deltaT; % Infiltration ventilation load  BTU/hr
U_walls_1_floor=0.073;
U_roof=0.049;
U_window=0.35; %%Low-e High solar
%      Areas, ft2
% South
SWalls=271.67+289.699; %ft2
SWindows=7.0486+19.3164;
Qload_south_walls=(SWalls-SWindows)*U_walls_1_floor*deltaT;
Qload_south_wind=SWindows*U_window*deltaT;
% East
EWalls=486.39837+95.2444;
EWindows=12.1528+43.5521+29.2917+20;
EDoors=42.25;
Qload_east_walls=(EWalls-EWindows-
EDoors)*U_walls_1_floor*deltaT;
Qload_east_wind=EWindows*U_window*deltaT;
% North
NWalls=527.6586+38.236;
Qload_North_walls=(NWalls)*U_walls_1_floor*deltaT;
% West
% Neglect garage
WWalls=468.733+79.9874+62.5;
WWindows=40+40;
WDoor=30;
Qload_West_walls=(WWalls-WWindows-
WDoor)*U_walls_1_floor*deltaT;
Qload_West_wind=WWindows*U_window*deltaT;
%Roof
U_roof=0.049;
Roof_Area=1655; % roof Area , ft2
deltaT_roof=68-((68-F(i))/2); %% Unheated attic mean T
between outside and inside T
Qload_roof=U_roof*Roof_Area*deltaT_roof;
%Total envelope loads
Qload=qvi+Qload_south_walls+Qload_south_wind+Qload_east_wal
ls+...
```

www.manaraa.com

```
    Qload_east_wind+Qload_North_walls+Qload_West_walls+...
    Qload_West_wind+Qload_roof;     %  Btu/hr
```

### A.8. Degree to radians conversion

```
function s = dr(d)
s = (pi/180) * d;
```

### A.9. Radians to degree conversion

```
function s = rd(d)
s = (180/pi) * d;
```

### A.10. Calculation of optimal degree for absorbed radiation.

```
function   Smax=optimal_beta_absorbed(beta,param,month)
m=month;
%Optimal angle for absorbed radiation
% Absorbed radiation
 Lat=param(1);
 Global(1:12)=param(2:13);
 Diffuse(1:12)=param(14:25);
 rho_g=[.7,.7,.7,.4,.2,.2,.2,.2,.2,.2,.4,.7,.7]; %Ground
reflectance (Assumed)
 N=1;%number of covers
l_g=0.0038; %glass thickness, m
KL=4*l_g;

[tau_alfa_g,tau_alfa_d,tau_alfa_b]=transmittence(beta,N,KL)
;
         if     m==1
             n=17;
         elseif m==2
             n=47;
         elseif m==3
```

www.manaraa.com

```
            n=75;
        elseif m==4
            n=105;
        elseif m==5
            n=135;
        elseif m==6
            n=162;
        elseif m==7
            n=198;
        elseif m==8
            n=228;
        elseif m==9
            n=258;
        elseif m==10
            n=288;
        elseif m==11
            n=318;
        elseif m==12
            n=344;
        end
    om1=acos(-tan(dr(Lat-beta ))*tan((sigma(n))));
    om2=acos(-tan(dr(Lat))*tan((sigma(n))));
    SUnset_angle_on_collec=min(om1,om2);
R_b(m)=(cos(dr(Lat-
beta))*cos(sigma(n))*sin(SUnset_angle_on_collec) +...
        SUnset_angle_on_collec*sin(dr(Lat-
beta))*sin(sigma(n)))/...

((cos(dr(Lat))*cos(sigma(n))*sin(SUnset_angle_on_collec))
+...

SUnset_angle_on_collec*sin(dr(Lat))*sin(sigma(n)));
Sbar=(Global(m)-
Diffuse(m))*R_b(m)*tau_alfa_b(m)+Diffuse(m)*tau_alfa_d*...

((1+cos(dr(beta)))/2)+Global(m)*tau_alfa_g*rho_g(m)*((1-
cos(dr(beta)))/2);
Smax=1/Sbar;
```

### A.10. Pump power calculation

```
function p=pump(rho,mwin,mu,pR,pD,Npump,pL)
Area=(pi*pD^2)/4;
V=mwin/rho/Area;
```

www.manaraa.com

```
Re=rho*V*pD/mu;
A=(2.457*log(1/((7/Re)^.9+.27*pR/pD)))^16;
B=(37530/Re)^16;
ff=8*((8/Re)^12+1/(A+B)^(3/2))^(1/12);
d=(ff*(pL/pD)*(1/2)*rho*V^2); %
p=(mwin*d)/(Npump*rho*1000);
```

www.manaraa.com

# Appendix B. Solar radiation data

## B.1. Diffuse radiation

```
2361770901002 595  502  648  469  314  154  530  254  478  391                02
2361770901002 298  394  473  656  451  456  410  427  344  296                03
2361770901002 435  458  201  275  261  285  446  253  414  210  467  12245    04
2361770901102                 247                           01
2361770901102 305  470  165  261  184  299  405  384  293  279                02
2361770901102  95  250  249  224  170  133  231  171  179  179                03
2361770901102 192  255  107  302  325  277  335  365  183  148   02   7415    04
2361770901202                 192                                           01
2361770901202 156  168  211  138  222  125   55   97  176  157                02
2361770901202 274  205  205  210  125  120  244  180  226  147                03
2361770901202 164  177  295  138  216  247  242  189  287  247  294   5937    04
2361770910102                 274                                           01
2361770910102 128  306  286  246  283  167  306  321  186  334                02
2361770910102 349  207   91  203  247  344  319  380  368  183                03
2361770910102 395  290  413  157  242  338  240  235  369  324  232   8489    04
2361770910202                 485                                           01
2361770910202 316  376  394  273  384  430  460  502  552  397                02
2361770910202 438  613  577  553  604  506  468  338  305  322                03
2361770910202 550  502  436  681  546  760  515  772    0    0    0  13570    04
2361770910302                 763                                           01
2361770910302 957  949  841  632  888  593  553  552  718  550                02
2361770910302 753  728  563  883  714  770  733  673 1007  727                03
2361770910302 774 1049 1065 1028  587  486  551  873  683  999   02  23642    04
2361770910402                 676                                           01
23617709104021012  844  403  913  419 1165  530  588  558  408                02
2361770910402 451  769  957  502  568  900  918  639  568  911                03
2361770910402 898  670  585  589  541  534  539  841  531  533    0  20284    04
2361770910502                 765                                           01
2361770910502 556  901  556  979 1033  983  726  663  696  802                02
2361770910502 690  981  957 1360 1208  750  901  620  763  564                03
2361770910502 664  485 1007  559  513  456 1056  574  567  472  662  23704    04
2361770910602                 861                                           01
2361770910602 657  830  461  428 1024  659  987  752 1107 1071                02
2361770910602 850 1008  795  828  677  968 1402  986 1025 1205                03
23617709106021053  943 1045  776  604  566  937  450  861  880    0  25835    04
2361770910702                 925                                           01
23617709107021208 1134 1143 1206  960  938  862  959  825 1029                02
2361770910702 955 1187  703  497  464  623  828 1237 1097 1176                03
2361770910702 738  962  759 1019  635  646  582  771 1144 1056 1333  28676    04
2361770910802                 735                                           01
2361770910802 677  723  938  655  929  866  823  744  487  915                02
2361770910802 682  986  885  858  507  911  907  986  592  625                03
2361770910802 863  631  581  414  549   02  762  841  469  702  556  22799    04
2361770910902                 533                                           01
2361770910902 750  708  646  232  835  525  653  785  397  405                02
2361770910902 876  529   02  490  512  525  402   02  325  354                03
2361770910902 510  514  339  378  388  585  649  584  630  408    0  16001    04
2361770911002                 426                                           01
2361770911002 265  419  459  318  572  387  369  552  648  618                02
2361770911002 508  513  237  648  470  620  523  396  526  407                03
2361770911002 544  309  429  227  335  285  292  460  328  300  256  13220    04
2361770911102                 289                                           01
2361770911102 500  351  166  443  454  290  287  295  258  218                02
2361770911102 176  267  234  279  292  241  304  207  346  245                03
2361770911102 216  254  260  391  185  293  228  362  308  312    0   8662    04
2361770911202                 221                                           01
2361770911202 283  120  122  288  237  308  166  193  282  180                02
```

www.manaraa.com

```
2361770911202 150  128  125  272  203  257  187  229  103  294                 03
2361770911202 247  232  263  251  236  213  247  273  243  256  277   6865    04
2361770920102                282                                              01
2361770920102 236  246  331  169  222  148  205  145  238  297                 02
2361770920102  81  237  266  316  354  272  366  355  334  257                 03
2361770920102 236  376  368  268  225  475  396  271  306  353  393   8742    04
2361770920202                489                                              01
2361770920202 359  335  545  391  349  341  451  439  418  379                 02
2361770920202 512  507  625  602  639  567  444  466  499  475                 03
2361770920202 411  457  623  478  208  669  777  584  618    0    0  14168    04
2361770920302                862                                              01
2361770920302 705  751  804  901  681 1095  710  883  964  752                 02
2361770920302 963  935  908  828  933 1005 1077  851  885  789                 03
2361770920302 900  832  839  740  804  768  754  952  759  993  950  26711    04
2361770920902                669                                              01
2361770920902 867  687  673  830  716  652  737  911  361  725                 02
2361770920902 804  638  535  725  801  566  870  775  836  345                 03
2361770920902 401  735  621  906  490  603  492  371  593  812    0  20078    04
2361770921002                493                                              01
2361770921002 383  777  446  455  667  594  552  658  453  445                 02
2361770921002 515  576  401  673  722  638  569  582  453  451                 03
2361770921002 342  449  561  397  359  351  237  395  209   02   02 15297    04
```

## B.2. Number of hours of sunshine

```
2361770690104                  930  30                                        01
2361770690204                 1270  45                                        01
2361770690304                 2060  66                                        01
2361770690404                 2000  67                                        01
2361770690504                 2340  75                                        01
2361770690604                 3440 115                                        01
2361770690704                 3300 106                                        01
2361770690804                 2770  89                                        01
2361770690904                 2390  80                                        01
2361770691004                  820  26                                        01
2361770691104                 1360  45                                        01
2361770691204                 1170  38                                        01

Skipping lines for years from 1970 to 1991

2361770920104                  800  26                                        01
2361770920204                 1790  62                                        01
2361770920304                 2200  71                                        01
2361770920804                 2720  88                                        01
2361770920904                 1260  42                                        01
2361770921004                 1980  64                                        01
```

## B.3. Global Radiation 1964 to 1991

```
2361770640501              2350                                               01
23617706405012679 2763 1821 1946 2666 2675 2817 2851 2620 2595                02
23617706405011180 2114 2901 1921 1071 2118 1980 1649 2524 1833                03
23617706405012733 2671 2474 2646 2809 1825 2541  983 3169 3098 3190  72850    04
2361770640601              2294                                               01
23617706406012855 2114 2097 2553 2181 3119 3131 1971 2700 1276                02
2361770640601 950 2285 1574 2491 3207 3161 2440 1620 2754 2189                03
23617706406012097 1842 1620 2038 2742 2574 2562 1942 2344 2411    02 68820    04
2361770640701              2502                                               01
```

www.manaraa.com

```
23617706407012436 2177 2775 2537 3286 2495 2784 2629 1649 2855                 02
23617706407011821 2867 2038 2600 2901 2934 2177 2193 3144 2738                 03
23617706407012909 2796 2696 2499 2763 1540 2466 2453 1967 2085 2352  77562    04
2361770640301               1281                                               01
23617706403011197  761 1268 1373 1318  686 1469 1565  937 1662                 02
23617706403011264  699 1699  841  711  418 1687 1607 1189 1909                 03
23617706403011925 1913 1858 1716  347  749  422 1369 1825 1800 1532  39711    04
2361770640401               1857                                               01
23617706404011000 1858 1632 2043 1105  975 1038 1557 1607 2064                 02
23617706404011147 2357 2281 2315 2105 2072 1708 2126 1900 2348                 03
23617706404012373 1875 1875 2281 2181  975 2369 1339 2600 2633    02 55710    04
2361770640501               2350                                               01
23617706405012679 2763 1821 1946 2666 2675 2817 2851 2620 2595                 02
23617706405011180 2114 2901 1921 1071 2118 1980 1649 2524 1833                 03
23617706405012733 2671 2474 2646 2809 1825 2541  983 3169 3098 3190  72850    04
2361770640601               2294                                               01
23617706406012855 2114 2097 2553 2181 3119 3131 1971 2700 1276                 02
2361770640601 950 2285 1574 2491 3207 3161 2440 1620 2754 2189                 03
23617706406012097 1842 1620 2038 2742 2574 2562 1942 2344 2411    02 68820    04
2361770640701               2502                                               01
23617706407012436 2177 2775 2537 3286 2495 2784 2629 1649 2855                 02
23617706407011821 2867 2038 2600 2901 2934 2177 2193 3144 2738                 03
23617706407012909 2796 2696 2499 2763 1540 2466 2453 1967 2085 2352  77562    04
2361770640801               2088                                               01
23617706408012742 1997 2683 2520 2399 2185 2302 2633 1448 2181                 02
23617706408012038 2302 2093 2252 2143 1122 2495 2486 2281 2156                 03
23617706408011285 1528 1398 2055 2185 2227 1498 2114 1532 2231 2244  64728    04
2361770640901               1484                                               01
23617706409012160  778 1934 2018 1050 1771 1963 1980 2055 1779                 02
23617706409011616 2030 1930 1783 1867 1934 1444 1147  397 1193                 03
2361770640901 406 1515 1712 1532 1507  619 1557 1674  607  573    02 44520    04
2361770641001                7511                                              01
23617706410011574 1452 1444 1457 1260 1327  422  259  699  628                 02
2361770641001 460  628  795 1080 10251 4771 2631 5101 69511076                 03
23617706410011029  351  460  180  364  464  347  519  690  715  648  232811   04
2361770641101               4631                                               01
2361770641101 519  280  410  142  803  837  774  644  745   66                 02
2361770641101 477  711  309  669  418  7411 5941 2301 1801 4011                 03
2361770641101 4351 452  1921  79  452  565  531  422  431  406    02 138901   04
2361770641201               305                                                01
2361770641201 418  154  163  154  263  150  351  414  498  230                 02
2361770641201 355  163  255  205  368  439  468  431  209  213                 03
2361770641201 251  259  188  263  167  159  473  355  506  594  339   9455    04
```

Skipping lines from 1965 to 1990

```
2361770910101               443                                                01
2361770910101 483  307  366  396  409  167  306  331  509  425                 02
2361770910101 434  208   91  433  247  426  368  529  534  571                 03
2361770910101 401  494  592  665  685  553  608  580  372  600  639  13729    04
2361770910201               775                                                01
2361770910201 720  715  634  744  690  524  637  502  676  844                 02
2361770910201 803  679  652  628  618  888  903 1081 1097 1095                 03
2361770910201 793  961  436 1093 1167  829  515  787    0    0    0  21711    04
2361770910301               1399                                               01
23617709103011023 1030  915 1287 1160 1472 1491 1517 1503 1559                 02
23617709103011553 1290 1606 1079 1547 1157  736 1387 1062  727                 03
23617709103011608 1530 1496 1595 1902 2020 1999 1699 1914 1109    02 43372    04
2361770910401               2026                                               01
23617709104011425 1942  403 1277 2181 1225  562 1885 2306 2310                 02
23617709104012371 2155 1407 2428 2326 1179 1920 2385 2418 2168                 03
23617709104012189 2412 2417 2508 2480 2449 2662 2126 2475 2801    0  60792    04
2361770910501               2515                                               01
23617709105012694  916 2627 2204 1862 2449 2738 2652 2708 2636                 02
23617709105012692 2502 2377 1915 1382 2762 1517 2774 2670 2898                 03
23617709105012841 2988 1745 2828 3034 3063 2242 3147 3087 3031 2987  77968    04
2361770910601               2619                                               01
23617709106012955 2593 3009 3086 2339 2862 2780 2755 1394 1979                 02
```

www.manaraa.com

```
23617709106013071 2146 2768 2560 3078 2632 1911 2578 1998 1921                03
23617709106012690 2515 2508 3033 3093 3116 2748 3161 2683 2596    0  78558    04
2361770910701               2290                                               01
23617709107012070 2579 2422 2547 2665 1107 2406 2669 2825 1403                02
23617709107012563 1273 2958 2865 3060 2928 2313 1584 2191 1772                03
23617709107012538 1681 1909 2638 2677 2631 2756 2610 1645 1774 1917  70976    04
2361770910801               1888                                               01
23617709108011120 1408 1931 2481 1141 2201 2335 2335 2622 2016                02
23617709108012240 2118 1827 2062 2449 2103 2137 1705 2333  706                03
2361770910801 989  632 2143 2185 2100    021791 1496 2038 1874 2112  58518    04
2361770910901               1440                                               01
23617709109011695  804 1928  232  907 1932 1826 1836 1930 1901                02
23617709109011182 1787    021806 1721 1594  653    021790 1711                03
23617709109011506 1512 1666 1653 1587 1101  737  823 1020 1466    0  43185    04
2361770911001                870                                               01
23617709110011497 1406 1238 1370 1191 1270 1232  580  937  715                02
2361770911001 510  634  237  816  610  691  973  983  933  961                03
2361770911001 574  309  917  991  787  948  950  753  765  300  877  26955    04
2361770911101                502                                               01
2361770911101 578  364  166  740  578  717  728  641  688  713                02
2361770911101 708  636  647  546  555  590  520  596  427  245                03
2361770911101 543  443  317  460  185  295  228  406  400  413    0  15073    04
2361770911201                309                                               01
2361770911201 348  120  122  288  402  348  166  193  445  456                02
2361770911201 150  128  125  311  445  270  197  371  103  403                03
2361770911201 439  444  385  356  433  447  433  277  411  274  280   9570    04
```

## B.4. Specifications for Form 4 and the File of Instantaneous Values of Direct Solar Radiation

| No. of record on MT, table line, punch card | Position No. | Number of positions | Content of record, table line, punch card | Comments |
|---|---|---|---|---|
| 1 | 2 | 3 | 4 | 5 |
| 1 | 1 | 1 | "4"- instantaneous values file identifier | |
| | 2-7 | 6 | Station synoptic index | |
| | 8-9 | 2 | Year | |
| | 10-11 | 2 | Month | |
| | 12-13 | 2 | Radiation parameter code | |
| | 14-16 | 3 | Degree \| station | |
| | 17-18 | 2 | Minutes \| latitude | |
| | 19-22 | 4 | Degrees \| station | |
| | 23-24 | 2 | Minutes \| longitude | |

www.manaraa.com

| | | | | |
|---|---|---|---|---|
| | 25-28 | 4 | Elevation above sea level (m) | |
| | 29 | 1 | Parameter T | Parameter T should take the following value : "0"-if the table indicates the true solar time of observation, "1"-if the sun's altitude is indicated |
| | 30-31 | 2 | Parameter L (the total number of lines filled up in a sheet ( or sheets) of Form 4 for the given station) | |
| | 32-78 | 47 | Blanks | |
| | 79-80 | 2 | "01" - the order number of record on MT, table line, punch card | |



| 1 | 2 | 3 | 4 | 5 |
|---|---|---|---|---|
| 2 | 1 | 1 | "4"- instantaneous values file identifier | |
| | 2-7 | 6 | Station synoptic index | |
| | 8-9 | 2 | Year | |
| | 10-11 | 2 | Month | |
| | 12-13 | 2 | Radiation parameter code | |
| | 14-15 | 2 | Date | |
| | 16-17<br>18-19 | 2<br>2 | Hours \| true solar<br>Minutes \| time of observation | |
| | | | or | |
| | 16-18 | 3 | the sun's altitude in 10th degrees | |
| | 19 | 1 | Parameter Z | Parameter Z can have the following values: "0"- if measurement was made before noon; "1" - at true noon; "2"- in the afternoon. |
| | 20-22 | 3 | Direct solar radiation value | |
| | 23 | 1 | Quality flag of direct solar radiation value | |
| | 24-27 | 4 | True solar time of observation or the sun's altitude | * |

www.manaraa.com

| | | | |
|---|---|---|---|
| 28-30 | 3 | Direct solar radiation value | |
| 31 | 1 | Quality flag | |
| 32-35 | 4 | True solar time of observation or the sun's altitude | * |
| 36-38 | 3 | Direct solar radiation value | |
| 39 | 1 | Quality flag | |
| . | . | | |
| . | . | | |
| . | . | | |

- 30 -

| 1 | 2 | 3 | 4 | 5 |
|---|---|---|---|---|
| | 64-67 | 4 | True solar time of observation or the sun's altitude | |
| | 68-70 | 3 | Direct solar radiation value | If less than 7 measurements were made during one day, the corresponding positions should not be filled in |
| | 71 | 1 | Quality flag | |
| | 72-78 | 7 | Blanks | |
| | 79-80 | 2 | "02" - the order number of record on MT, table line, punch card | |
| | . | . | | The order number of the last record should be equal to parameter value L (see record 1) |
| | . | . | | |
| | . | . | | |

* Positions are filled in similarly to positions 16-19.

## B.5. Specifications for Forms 1A & IB and Description File

| No.of record on MT, table line, punch | Position No. | Number of positions | Content of record,table line, punch card | Comments |
|---|---|---|---|---|

www.manaraa.com

| card | | | | |
|---|---|---|---|---|
| 1 | 2 | 3 | 4 | 5 |
| 1 | 1 | 1 | "1" - description file identifier | |
| | 2-7 | 6 | Station synoptic index | For stations with the WMO synoptic index, bytes 2-6 are filled in, byte 7 is filled in with zero; the six-digit index assigned by the WRDC is recorded in positions 2-7 |
| | 8-9 | 2 | Year | The last two figures of the year are recorded |
| | 10-11 | 2 | The number of lines filled up in a sheet (or sheets) of Form 1A (parameter LA) | |
| | 12-13 | 2 | The total number of lines filled up in sheets Forms 1A and 1B (parameter LB) | |
| | 14-16<br>17-18 | 3<br>2 | Degrees \| station<br>Minutes \| latitude | The sign "-" means the southern hemisphere |
| | 19-22<br>23-24 | 4<br>2 | Degrees \| station<br>Minutes \| longitude | The sign "-" means the western hemisphere |
| | 25-28 | 4 | Station elevation above sea level (m) | |
| | 29-78 | 50 | Blanks | |



| 1 | 2 | 3 | 4 | 5 |
|---|---|---|---|---|
| | 79-80 | 2 | "01" - the order number of record on MT, table line, punch card | |
| 2 | 1 | 1 | "1" - description file identifier | |
| | 2-7 | 6 | Station synoptic index | |
| | 8-9 | 2 | Year | |
| | 10-22 | 13 | Reference instrument type | Plain language |

www.manaraa.com

| | | | | |
|---|---|---|---|---|
| | 23-32 | 10 | Series number of reference instrument | |
| | 33-40 | 8 | Calibration factor of reference instrument | |
| | 41-56 | 16 | Units of calibration factor | Plain language |
| | 57-60<br>61-62<br>63-64 | 4<br>2<br>2 | Year<br>Month<br>Day<br>Date of reference instrument calibration | |
| | 65-78 | 14 | Place of reference instrument calibration | Plain language |
| | 79-80 | 2 | "02" - the order number record, table line, punch card | |
| 3 | 1 | 1 | "1" - description file identifier | |
| | 2-7 | 6 | Station synoptic index | |
| | 8-9 | 2 | Year | |
| | 10-78 | 69 | Station history - comments on different changes at station | Plain language |



| 1 | 2 | 3 | 4 | 5 |
|---|---|---|---|---|
| | 79-80 | 2 | "02" - the order number of record on MT, table line, punch card | The number of these records is equal to the number of "comments" lines and is variable |
| LA+1 | 1 | 1 | "1"- description file identifier | The beginning of Form 1B records |
| | 2-7 | 6 | Station synoptic index | |
| | 8-9 | 2 | Year | |
| | 10-11 | 2 | Code of radiation parameter | |
| | 12,13,14 | 3 | Codes of the time resolution of parameter measured | |
| | 15-40 | 26 | Instrument type | The receiving surface colour can be indicated,e.g. "black and white pyranometer" |
| | 41-50 | 10 | Instrument series, | |

www.manaraa.com

| | | | | |
|---|---|---|---|---|
| | | | number | |
| | 51-66 | 16 | Manufacturer | |
| | 67-70 | 4 | Instrument manufacturer year | |
| | 71-72<br>73-74 | 2<br>2 | Year \| Beginning of<br>Month \| measurements<br>\| with the in-<br>\| strument | |
| | 75-76<br>77-78 | 2<br>2 | Year \| Discontinuance<br>Month \| of measurements<br>\| with the instru-<br>\| ment | |
| | 79-80 | 2 | The order number of record on MT, table line, punch card | |
| LA+2 | 1 | 1 | "1"- description file identifier | |

- 16 -

| 1 | 2 | 3 | 4 | 5 |
|---|---|---|---|---|
| | 2-7 | 6 | Station synoptic index | |
| | 8-9 | 2 | Year | |
| | 10-11 | 2 | Code of radiation parameter | |
| | 12-24 | 8 | Calibration factor before the first calibration in the given year | |
| | 25-39 | 15 | Units | Plain language |
| | 40-41<br>42-43 | 2<br>2 | Month \| Date of the<br>Day \| 1st calibrati-<br>\| on in the gi-<br>\| ven year | |
| | 44 | 1 | Calibration type | 1 - calibration by the sun<br>2 - calibration by lamp |
| | 45-52 | 8 | Calibration factor | |
| | 53-54<br>55-56 | 2<br>2 | Month \| Date of the se-<br>Day \| cond calib-<br>\| ration | If the 2nd and the 3rd calibrations were not made, the position are not filled in |
| | 57 | 1 | Calibration type | |
| | 58-65 | 8 | Calibration factor | |

www.manaraa.com

| | | |
|---|---|---|
| 66-67 | 2 | Month \| Date of the |
| 68-69 | 2 | Day \| 3rd calibra- |
| | | \| tion |
| 70 | 1 | Calibration type |
| 71-78 | 8 | Calibration factor |
| 79-80 | 2 | The order number of re- cord on MT, table line, punch card |

- 17 -

## B.6. 4.2. Specifications for Form 2 and Daily Sums File

| No.of record on MT, table line, punch card | Position No. | No.of positions | Content of record, table line, punch card | Comments |
|---|---|---|---|---|
| 1 | 2 | 3 | 4 | 5 |
| 1 | 1 | 1 | "2"- daily sums file identifier | |
| | 2-7 | 6 | Station synoptic index | |
| | 8-9 | 2 | Year | |
| | 10-11 | 2 | Month | |
| | 12-13 | 2 | Radiation parameter code | |
| | 14-16 | 3 | Degrees \| station | The sign "-" means the southern hemisphere |
| | 17-18 | 2 | Minutes \| latitude | |
| | 19-22 | 4 | Degrees \| station | The sign "-" means the western hemisphere |
| | 23-24 | 2 | Minutes \| longitude | |
| | 25-28 | 4 | Station elevation above sea level (m) | |
| | 29-32 | 4 | Monthly mean of daily sums | |
| | 33 | 1 | Quality flag of monthly mean of daily sums | |
| | 34-37 | 4 | Monthly sum of sunshine duration | |
| | 38 | 1 | Quality flag of monthly sum of sunshine duration | |
| | 39-41 | 3 | Monthly mean of sunshine duration | |
| | 42 | 1 | Quality flag of monthly mean of sunshine duration | |
| | 79-80 | 2 | "01"- the order number of record on MT, table line, punch card | |

www.manaraa.com

| | | | |
|---|---|---|---|
| 2 | 1 | 1 | "2"- daily sums file identifier |
| | 2-7 | 6 | Station synoptic index |
| | 8-9 | 2 | Year |
| | 10-11 | 2 | Month |
| | 12-13 | 2 | Radiation parameter code |
| | 14-17 | 4 | Daily sum for the 1st day of the month |

- 18 -

| 1 | 2 | 3 | 4 | 5 |
|---|---|---|---|---|
| | 18 | 1 | Quality flag of daily sum for the first day | |
| | 19-22 | 4 | Daily sum for the second day of the month | |
| | 23 | 1 | Quality flag of daily sum for the second day | |
| | . | . | | |
| | . | . | | |
| | . | . | | |
| | 59-62 | 4 | Daily sum for the 10th day of the month | |
| | 63 | 1 | Quality flag of daily sum for the 10th day | |
| | 64-78 | 15 | Blanks | |
| | 79-80 | 2 | "02"- the order number of record on MT Table line, punch card | |
| 3 | 1 | 1 | "2"- daily sums file identifier | |
| | 2-7 | 6 | Station synoptic index | |
| | 8-9 | 2 | Year | |
| | 10-11 | 2 | Month | |
| | 12-13 | 2 | Radiation parameter code | |
| | 14-17 | 4 | Daily sum for the 11th day of the month | |
| | 18 | 1 | Quality flag of daily sum for the 11th day | |
| | 19-22 | 4 | Daily sum for the 12th day of the month | |
| | 23 | 1 | Quality flag of daily sum for the 12th day | |
| | . | . | | |
| | . | . | | |
| | . | . | | |

- 19 -

www.manaraa.com

| 1 | 2 | 3 | 4 | 5 |
|---|---|---|---|---|
| | 59-62 | 4 | Daily sum for the 20th day of the month | |
| | 63 | 1 | Quality flag of daily sum for the 20th day | |
| | 64-78 | 15 | Blanks | |
| | 79-80 | 2 | "03" - the order number Or record on MT, table line, punch card | |
| 4 | 1 | 1 | "2" - daily sums file identifier | |
| | 2-7 | 6 | Station synoptic index | |
| | 8-9 | 2 | Year | |
| | 10-11 | 2 | Month | |
| | 12-13 | 2 | Radiation parameter code | |
| | 14-17 | 4 | Daily sum for the 21st day of the month | |
| | 18 | 1 | Quality flag of daily sum for the 21st day | |
| | . | . | | |
| | . | . | | |
| | . | . | | |
| | 64-67 | 4 | Daily sum for the 31st day of the month | |
| | 68 | 1 | Quality flag of daily sum for the 31st day | |
| | 69-74 | 6 | Monthly sum | |
| | 75 | 1 | Quality flag of monthly sum | |
| | 76-78 | 3 | Blanks | |
| | 79-80 | 2 | "04" - the order number of record on MT, table line, punch card | |

www.manaraa.com

## Appendix C. G series Solar Collectors

| Product # | Description | Retail |
|---|---|---|
| G32-P | 4' x 8' Grid collector, 3/4" hdr, selective paint | $840 |

## A. General Information

### 1.0 Product Description:

Thermo Dynamics G Series flat plate liquid collectors are single glazed with low-iron tempered glass. The absorber is an arrangement of parallel riser fins connected to top and bottom headers. The fins are aluminum with integral copper riser tubes, which are completely surrounded by the aluminum and are metallurgically bonded together. The copper riser tubes are soldered to internal manifolds (headers), which are available in either 3/4" or 1" diameter copper pipe. The back and sides are insulated with a 25 mm (1") layer of compressed fiberglass. The collector frame is extruded aluminum with a baked-enamel finish, (dark brown). Collector mounting is by way of a sliding bolt-track. Flush and racked collector mounting formats are easily accommodated.

### 1.1 Options

Factory installed temperature sensors; 3/4" and 1" headers; 12 mm (1/2") riser tubes; absorber coatings: selective Anodic-Cobalt surface, or selective paint surface.

### 1.2 Dimensions and Volumes

1.20 m x 2.47 m x 0.086 m

(47-3/8 in x 97-3/8 in x 3-3/8 in)
Gross area: 2.96 m2 (31.9 ft2)
Aperture area: 2.78 m2 (30.0 ft2)
Absorber area: 2.87 m2 (30.9 ft2)
Volume (19 mm (3/4") header): 1.84 liter (0.40 IG) Volume (25 mm (1") header): 2.40 liter (0.53 IG)

### 1.3 Weight:

www.manaraa.com

Net: 45 kg (99 lb)
Shipping: 64 kg (140 lb)
(includes wooden crate)

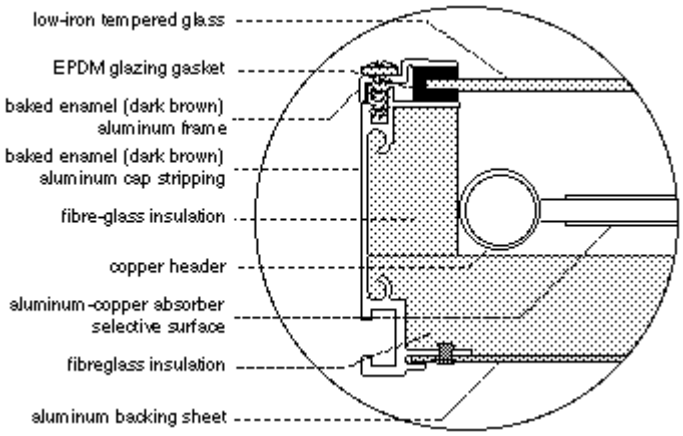


## 2.0 Product Use

### 2.1 Product Applications:

Residential and commercial domestic hot water, process hot water, space heating, pool heating

### 2.2 Geographic and Climatic Limitations:

None.

## 3.0 Manufacturer's Experience

### 3.1 Background

Thermo Dynamics Ltd. (TDL) is a Canadian company engaged in the research, development, production, distribution and installation of solar thermal equipment. The company has been involved in the solar thermal industry since 1981 and operates from its head office and factory in Dartmouth, Nova Scotia, Canada, the sister city of Halifax situated on the Atlantic coast. The company's specialization is the glazed liquid-flat-plate (LFP) collectors with metal absorbers. TDL is a fully integrated solar thermal company with the ability to convert raw aluminum and copper into a high technology solar water heating system.

Thermo Dynamics Ltd., as a world leader in solar technology, manufactures and markets solar heating equipment from

www.manaraa.com

complete systems to basic selective surface components for O.E.M.'s licensees, dealers and distributors through out North America, Europe, Africa, New Zealand, as well as 10 other countries around the world.

**3.2 Production:**

3000 m2 per year for G32 collectors.

**3.3 Projects:**

Mount Saint Vincent Motherhouse, Halifax, Nova Scotia, Canada. Largest SDHW system in Canada. Collector type and number: 224 - G32 Collector area: 675 m2 (7,265 ft2) 1.75 GJ/m2 /year (154 MBtus/ft2 /year)
Top of the Mountain Apartments, Halifax, Nova Scotia, Canada. Collector type and number: 49 - G32; 49 - G40 Collector area: 328 m2 (3,531 ft2) 1.78 GJ/m2 /year (156 MBtus/ft2 /year)

Somerset Place Apartments, Halifax, Nova Scotia, Canada Collector type and number: 120 - G32 Collector area: 356 m2 (3,332 ft2) 2.10 GJ/m2 /year (185 MBtus/ft2 /year)

Thermo Dynamics Ltd. has installed thousands of solar residential domestic hot water and pool heating systems.

---

## B. Glazing System

**1.0 General Description:**

Glazing is a 3.2 mm (1/8") single sheet of low-iron tempered glass with an EPDM rubber seal around the edges. Glazing is secured by an aluminum capping fastened by stainless steel screws around the perimeter.

**1.1 Trade Names:**

Solite

**1.2 Chemical Composition:**

Iron oxide content of 0.03%

**1.3 Physical Treatment:**

www.manaraa.com

All glazing is tempered with swiped edges and has a shallow stipple pattern to reduce specular reflectance.

**1.4 Thickness:**

3.18 mm (1/8")

**1.5 Spacing:**

Glazing to absorber: 20 to 25 mm (3/4" to 1")

**1.6 Weight:**

7.8 kg/m2 (1.6 lb/ft2)

**1.7 Appearance:**

Translucent; the inner surface is embossed with a stipple pattern which produces a frosted effect.

**2.0 Optical Performance**

**2.1 Spectral Transmittance:**

Visible light 89.8% ASTM E424-71A Ultra violet light 51% ISO 9050 Solar light/energy 89.5% ASTM E424-71A

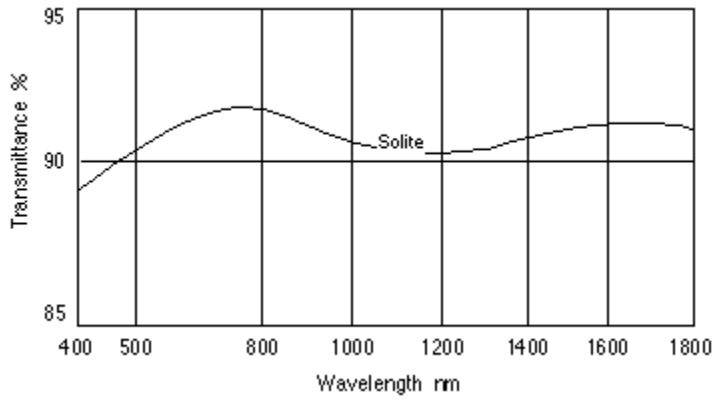


**2.2 Energy Transmission:**

Solar spectrum (0-3 micrometres) 89.5% Infrared spectrum (>3 micrometres) No data available

**2.3 Refractive Index:**

1.525

**3.0 Structural Performance**

**3.1 Tensile Strength:**

www.manaraa.com

Design Pressure is 2.87 kPa (.416 psi) for 1/8 inch glass with a design factor of 2.5. Tensile strength is 152 MPa (22,000 psi) with a 2.5 safety factor.

**3.2 Impact Resistance:**

Glazing can withstand 542 J (400 ft-lb) soft-body impact, 3 to 5 times stronger than annealed glass.

**3.3 Uniform Load Resistance:**

Uniform load testing was conducted at the National Solar Test Facility in May1986 as part of CSA-378. Positive load: 1.5 kPa (0.22 psi) Negative load: 1.9 kPa (0.28 psi)

**4.0 Thermal Performance**

**4.1 Coefficient of Thermal Expansion:**

89.9 x 10-7 1/°C (49.9 x 10-7 1/°F)

**4.2 Operating Temperature Range:**

Min: below -46°C (-51°F); max: 260°C (500°F)

**4.3 Thermal Conductivity:**

No data available

**5.0 Fire Behavior:**

Non-combustible. Does not produce toxic fumes in a fire situation.

**6.0 Durability:**

Glass is chemically inert to most chemical solvents and staining agents, and is resistant to surface weathering, ultraviolet and thermal degradation, and moisture damage.

---

## C. Absorber System

**1.0 General Description:**

The absorber consists of eight parallel aluminum fins with integral copper riser tubes, which are bonded to and completely surrounded by the aluminum by means of high-pressure cold-rolling process. The absorber coating is Anodic-Cobalt selective surface or black paint selective surface. The riser/header connection has two parts, a short copper nipple brazed to the header with the absorber fin soldered to the copper nipple.

www.manaraa.com

## 1.1 Generic/Trade Names:

Absorber fins: "Sunstrip"
Tubes: copper
Headers: Type M copper
Coating: selective Anodic-Cobalt or paint
Solder/Brazing: 95/5 tin antimony/Silfos

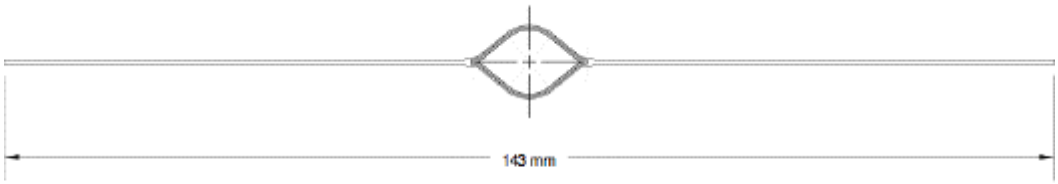


scale: 1:1 mm

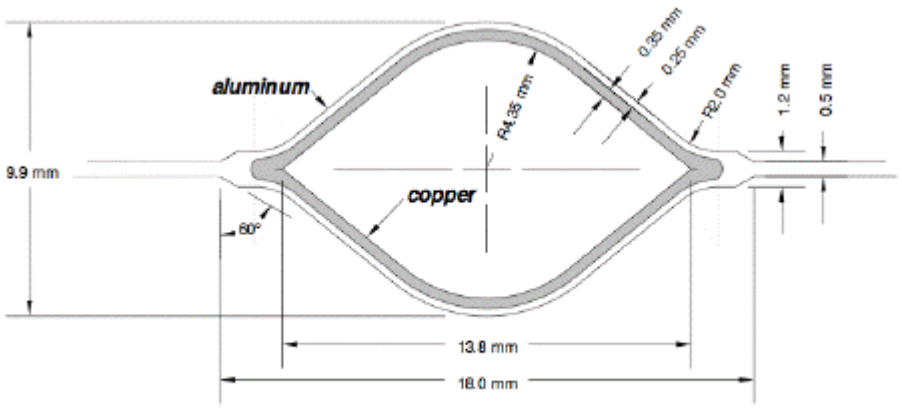


scale: 4:1 mm

## 1.2 Chemical Composition:

Absorber fins: aluminum (AA 1350/0 alloy)
Tubes: copper (CDA 1220/0 alloy)
Headers: copper
Coating: anodized-cobalt pigmented, or semi-selective paint
Solder/Brazing: no data available

## 1.3 Physical Treatment:

None.

## 1.4 Dimensions:

www.manaraa.com

Tube diameter: rhombic shape with an open area of about 120 mm2 (0.19 in2 )
Tube spacing: 143 mm (5.63")
Header diameter: 22.2 or 28.6 mm (3/4" or 1") nominal
Absorber thickness: 0.5 mm (0.02")
Coating thickness: no data available.

**2.0 Optical Performance**

**2.1 Absorptivity of Solar Radiation:**

Painted surface: a = 95%
Anodic-Cobalt surface: a = 92%

**2.2 Emissivity of Infrared Radiation:**

Painted surface: e = 25%
Anodic-Cobalt surface: e = 15%

**3.0 Thermal Performance**

**3.1 Thermal Transfer:**

Good thermal transfer due to the high conductivity of aluminum and the bond between the aluminum fins and copper tubes.

**3.2 Coefficient of Thermal Expansion:**

Absorber: no data available
Tubes: no data available

To allow for thermal expansion, the absorber is free to float within the collector container. EPDM gaskets prevent contact between the copper headers and the aluminum container.

**3.3 Thermal Capacity of Absorber System:**

No data available.

**3.4 Operating Temperature Range:**

Absorber: max. 300°C (572°F)
Tubes: max. 300°C (572°F)
Solder/Brazing: min. -50°C (-58°F); max. 400°C (752°F)
Coating: max. 300°C (572°F)

**4.0 Mechanical Integrity:**

The collector has completed 30-day stagnation testing at The National Solar Test Facility (NSTF), Mississauga, Canada, with no sign of degradation or loss in performance.

**5.0 Durability:**

www.manaraa.com

The absorber and the selective surface are not affected by normal aqueous solutions. Stagnation testing has shown no thermal degradation.

---

## D. Insulation

### 1.0 General Description:

Collectors are insulated around the sides and back with fiberglass board. Complies with ASTM-C-612 Classes 1 and 2.

### 1.1 Trade Names:

Sides: Fiberglas AF530
Back: Fiberglas AF530

### 1.2 Chemical Composition:

Fibrous glass bonded by a thermosetting resin. Inorganic, will not rot.

### 1.3 Density:

48 kg/m3 (3.0 lb/ft3)

### 1.4 Thickness:

Side: 25 mm (1")
Back: 25 mm (1")

### 2.0 Thermal Performance

### 2.1 Thermal Conductivity:

0.036 W/m·°C (0.25 Btu ·in/hr·ft2·°F) at 24°C (75°F)

### 2.2 Thermal Resistance:

RSI 0.7 °C·m2/W (R 4 °F·ft2·hr/Btu) at 24°C (75°F)

### 2.3 Coefficient of Thermal Expansion:

No data available

### 2.4 Operating Temperature Range:

Maximum continuous operating temperature is 232°C (450°F).

### 3.0 Fire Behavior

### 3.1 Surface Burning Characteristics:

Fiberglas AF530 is inherently fire safe. ULC Flame Spread rating of 15. (compared to untreated Red Oak as 100 - test method ULC S-102)

www.manaraa.com

**4.0 Durability:**

No changes should occur to the insulation when subjected to chemicals normally encountered in use conditions. No thermal degradation has been found after prolonged stagnation testing. Moisture adsorption is less than 0.2% by volume, 96 hours at 49°C (120°F) and 95% R.H. Inorganic therefore does not breed or promote bacteria and fungus. Essentially odorless.

www.manaraa.com

# STEP 1: Known Operating Parameters

Unit Conversions

| From | To | Multiply by |
|---|---|---|
| kW | MBtu/hr | 3.4123 |
| IGPM | USGPM | 1.2 |
| kg/s | IGPM | 13.19 |
| °C | °F | 1.8 |

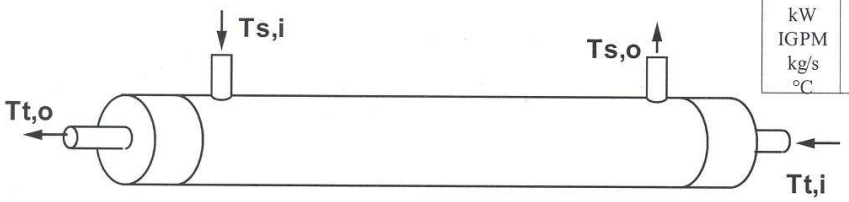


**Consider the following when allocating the heat transfer fluids:**

- Fluids under high pressure and/or corrosive fluids are generally circulated through the tube side.
- Chemical cleaning is recommended. Mechanical cleaning is not possible with DTL Series heat exchangers.
- High viscosity fluid should be circulated on the shell side. Propylene glycol, for example, has higher viscosity than water.
- Head loss on the tube side of the heat exchanger is generally ten times less than the shell side head loss for equal flow rates.

**1.1** Make a note of the following parameters in the boxes provided on the Worksheet.

Shell Side Inlet Temperature, **Ts,i**
Tube Side Inlet Temperature, **Tt,i**
Heat Transfer Load, **Q**
Shell Side Outlet Temperature, **Ts,o**
Tube Side Outlet Temperature, **Tt,o**

**1.2**

Use the figures given here to determine Ts,o and Tt,o from the flow rate or vice versa. The figures are for water as the working fluid.

For 50/50 or 40/60 propylene glycol/water mixtures multiply (To-Ti) by 1.1.

If To - Ti gives a negative result then simply drop the negative sign when using the graphs at the right.

Always operate within the range of parameters provided. This will ensure that flow is turbulent but not excessively noisy.

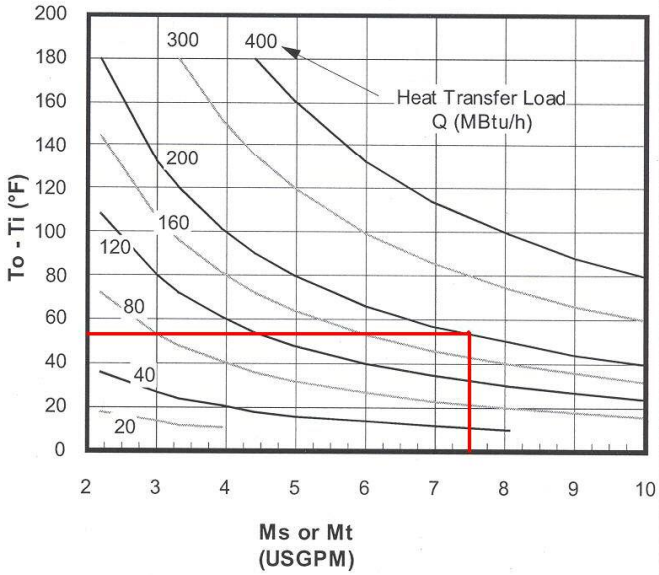


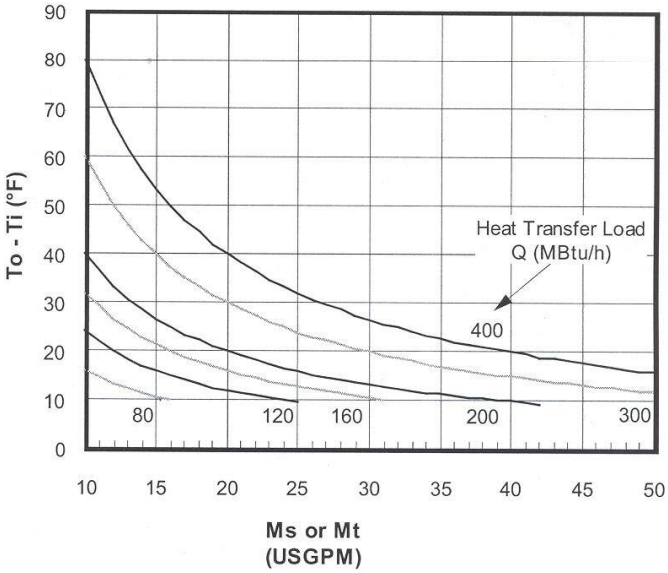


www.manaraa.com

# STEP 2: The Overall Heat Transfer Coefficient

Unit Conversions

| From | To | Multiply by |
|---|---|---|
| IGPM | USGPM | 1.2 |
| Btu/h-ft2-°F | W/m2-K | 5.68 |

**2.1** Estimate the Degree of Fouling:

**Light Fouling** - Distilled water

**Moderate Fouling** - Treated boiler feedwater, below 120°F (50°C)

**Heavy Fouling** - Treated boiler feedwater above 120°F (50°C), River water, Well water, propylene glycol /water.

**2.2**

Estimate the overall heat transfer coeffient, U, from the appropriate graph using the shell side flow rate, Ms. Two cases are presented (A and B). Both are valid for forced circulation on the shell and tube sides only.

If the hotter fluid is circulated on the tube side, then increase U by 10%.

Make a note of U in the box provided on the Worksheet.

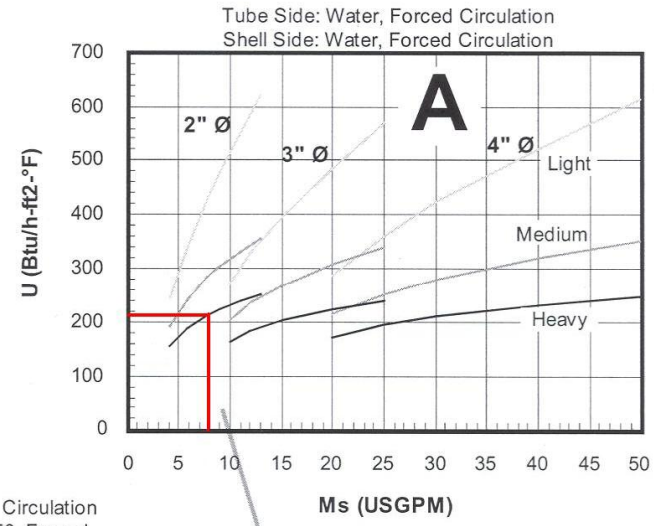


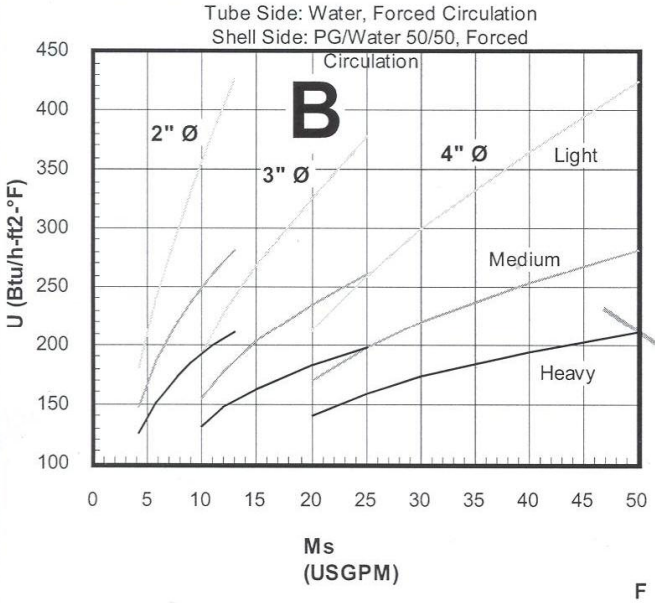


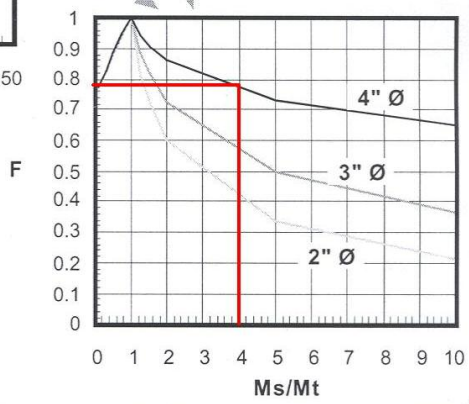


**2.3** Calculate the ratio of shell side to tube side flow rates, Ms/Mt.

**2.4** Estimate the factor, F, using the flow rate ratio and make a note in the box provided on the Worksheet.



www.manaraa.com

## STEP 3: Log Mean Temperature Difference

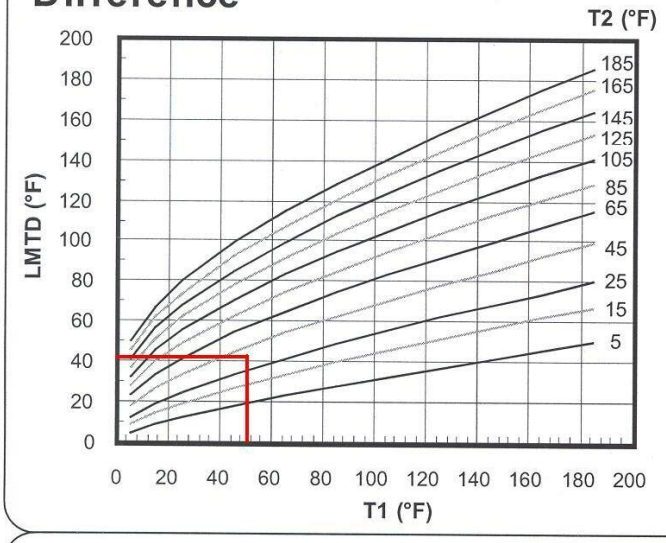


Unit Conversions

| From | To | Multiply by |
|---|---|---|
| °C | °F | 1.8 |

**3.1** Calculate T1 and T2 using the equations provided on the Worksheet.

If the above calculations result in a negative value for T1 and/or T2 then simply drop the negative sign prior to using the graph at the right.

**3.2** Estimate LMTD from the graph. Make a note of LMTD in the box provided on the Worksheet.

## STEP 4: Heat Exchanger Length

Unit Conversions

| From | To | Divide by |
|---|---|---|
| m | ft | 0.3048 |
| m2 | ft2 | 0.0929 |

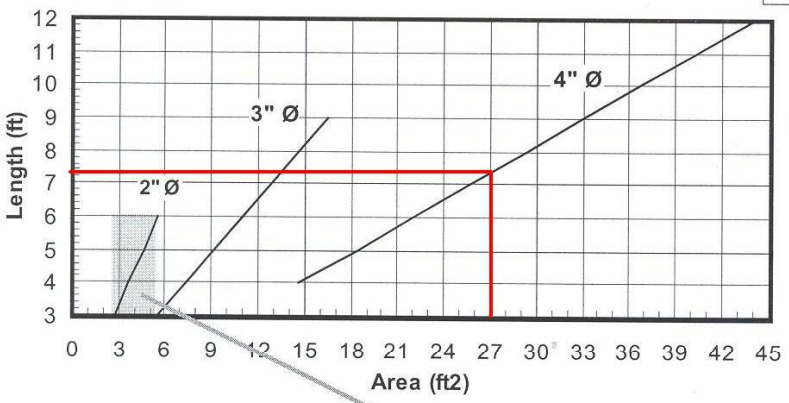


$$A = \frac{Q \times 1000}{F \times U \times LMTD}$$

**4.1** Calculate the required heat exchanger area using the formula given above. Record the result in the box provided on the Worksheet.

**4.2** Use the heat exchanger area, A, and shell diameter, to determine the heat exchanger length from the appropriate graph. Record the heat exchanger length in the box provided on the Worksheet.

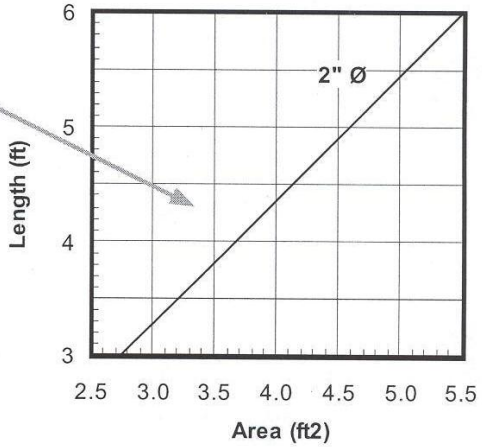




www.manaraa.com

Date: File number:

Job Number: Sized By:

# DTL WORKSHEET

Use this page to record the various parameters that are found throughout the procedure. Photocopy this page and keep it as a permanent copy of the sizing information.

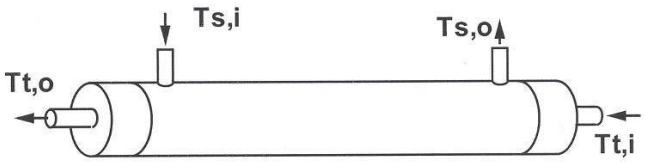


| Known Operating Parameters | | | Section | Results | | |
|---|---|---|---|---|---|---|
| Ts,i | 150 | °F | 2.2 or 2.3 | U | 225 | Btu/h-ft2-°F |
| Tt,i | 68 | °F | | Ds | 4 | inches |
| Q | 200 | MBtu/h | 2.4 | Ms/Mt | 4 | |
| Ts,o | 98 | °F | 2.5 | F | 0.8 | |
| Tt,o | 120 | °F | 3.1 | T1 = Ts,i - Tt,o | 52 | °F |
| Ms | 8 | USGPM | 3.1 | T2 = Ts,o - Tt,i | 30 | °F |
| Mt | 2 | USGPM | 3.2 | LMTD | 40 | °F |
| | | | 4.1 | Area | 27 | ft2 |
| | | | 4.2 | Length | 8 | ft |

## Operating Costs:

**Power** Consumption = $\frac{Ms \times Hs}{5.29} + \frac{Mt \times Ht}{5.29} = \frac{\square \times \square}{5.29} + \frac{\square \times \square}{5.29} =$ Watts

**Hours** of Pump Operation per Year

kWh/yr = **Power** Consumption x Hours / 1000

$/kWh **Electrical** Energy Cost

$/Year = $/kWh x kWh/Year

Note that there are generally several heat exchangers that will satisfy the given operating conditions. The heat exchanger that gives the lowest overall total cost should be selected. Remember that the cost of the pump and installation must be considered in the overall cost of the heat exchanger. Cost of pumping through connecting pipe must also be considered.

### Standard Sizes Available

| Shell Diameter (in) | Number of Tubes | Shell Lengths Available (ft) |
|---|---|---|
| 2 | 7 | 3,4,6,8 and 9 |
| 3 | 14 | 3,4,6,8 and 9 |
| 4 | 28 | 4,6,8,9 and 12 |

Special orders available upon request.

**PLACING AN ORDER:**
Specify the model number in the spaces provided.

Contact Thermo Dynamics Ltd. at
Tel. (902) 468-1001
Email: thermody@atcom.com
Facsimile (902) 468-1002

**Quantity** ___ **Model D** ___**T** ___**L** ___

www.manaraa.com

## Appendix D. Building envelope surfaces areas.

Table D.1: South elevation

| Angle / Surface | 90° | 27° |
|---|---|---|
| Walls | 271.67'<br>289.699' | |
| Windows | 7.0486'<br>19.3164' | |
| Roof | | 106' |

Table D.2: East elevation

| Angle / Surface | 90° | 27° |
|---|---|---|
| Walls | 486.39837'<br>95.2444' | |
| Windows | 12.1528'<br>43.5521'<br>29.2917<br>20' | |
| Door | 42.25' | |
| Roof | | 15809.2093'<br>174.133' |

www.manaraa.com

Table D.3: North elevation

| Angle / Surface | 90° | 27° |
|---|---|---|
| Walls<br>Brick wall | 527.6586 '<br>38.236' | |
| Roof | | 30.23'<br>149.19' |

Table D.4: West elevation

| Angle / Surface | 90° | 27° |
|---|---|---|
| Walls | 468.733'<br>79.9874' | |
| Brick wall | 62.5' | |
| Windows | 40'<br>40' | |
| Door | 30' | |
| Garage doors | 112'<br>60' | |
| Part of the garage wall | 95.8'<br>33.7' | |
| Roof | | 249.7'<br>535.394'<br>412.438' |

www.manaraa.com

## Appendix E. Climate data

The climate data retrieved from www.worldclimate.com which has been derived from GHCN 1: The Global Historical Climatology Network version 1 and from GHCN 2 Beta: The Global Historical Climatology Network, version 2 beta respectively.

Weather station Celinograd (Astana) is at about 51.13°N 71.30°E.

Table E.1: 24-hr Average Temperature

| | Jan | Feb | Mar | Apr | May | Jun | Jul | Aug | Sep | Oct | Nov | Dec | Year |
|---|---|---|---|---|---|---|---|---|---|---|---|---|---|
| °C | -16.7 | -16.5 | -10.1 | 2.9 | 12.9 | 18.5 | 20.7 | 17.9 | 11.4 | 2.5 | -6.9 | -13.8 | 2.0 |
| °F | 1.9 | 2.3 | 13.8 | 37.2 | 55.2 | 65.3 | 69.3 | 64.2 | 52.5 | 36.5 | 19.6 | 7.2 | 35.6 |

Source: CELINOGRAD data derived from GHCN 2 Beta. 1191 months between 1881 and 1989

Table E.2: Average Maximum Temperature

| | Jan | Feb | Mar | Apr | May | Jun | Jul | Aug | Sep | Oct | Nov | Dec | Year |
|---|---|---|---|---|---|---|---|---|---|---|---|---|---|
| °C | -12.0 | -11.3 | -4.7 | 9.2 | 19.5 | 25.2 | 27.0 | 24.5 | 18.6 | 8.6 | -2.9 | -9.8 | 7.7 |
| °F | 10.4 | 11.7 | 23.5 | 48.6 | 67.1 | 77.4 | 80.6 | 76.1 | 65.5 | 47.5 | 26.8 | 14.4 | 45.9 |

Source: CELINOGRAD data derived from GHCN 2 Beta. 817 months between 1900 and 1989

Table E.3: Average Minimum Temperature

| | Jan | Feb | Mar | Apr | May | Jun | Jul | Aug | Sep | Oct | Nov | Dec | Year |
|---|---|---|---|---|---|---|---|---|---|---|---|---|---|
| °C | -21.6 | -21.5 | -15.2 | -2.2 | 5.8 | 11.3 | 13.5 | 11.0 | 5.2 | -1.9 | -11.1 | -18.4 | -3.6 |
| °F | -6.8 | -6.6 | 4.6 | 28.0 | 42.4 | 52.3 | 56.3 | 51.8 | 41.4 | 28.6 | 12.0 | -1.0 | 25.5 |

www.manaraa.com

Source: CELINOGRAD data derived from GHCN 2 Beta. 1143 months between 1884 and 1989

Table E.4: Average Rainfall

| | Jan | Feb | Mar | Apr | May | Jun | Jul | Aug | Sep | Oct | Nov | Dec | Year |
|---|---|---|---|---|---|---|---|---|---|---|---|---|---|
| mm | 14.9 | 13.1 | 14.6 | 16.8 | 28.5 | 37.4 | 47.2 | 35.7 | 23.1 | 23.8 | 16.5 | 14.5 | 287.5 |
| inches | 0.6 | 0.5 | 0.6 | 0.7 | 1.1 | 1.5 | 1.9 | 1.4 | 0.9 | 0.9 | 0.6 | 0.6 | 11.3 |

Source: CELINOGRAD data derived from GHCN 1. 1196 months between 1881 and 1990

www.manaraa.com